Simulation and modeling of nonlinear mirror modes

P.L. Sulem, T. Passot
CNRS, Observatoire de la Côte d'Azur, Nice

P. Hellinger, P. Travnicek
Institute of Atmospheric Physics, Prague

E. Kuznetsov
Lebedev Physical Institute and
Space Research Institute, Moscow

F. Califano
Dipartimento di Fisica, Universita' di Pisa

WPI, Vienna, 16-20 February 2009

Outline

- Satellite observations
- Vlasov-Maxwell simulations of the mirror instability
  and of its nonlinear developments: magnetic “holes” or “humps”
- Theoretical interpretations
- Bistability: Magnetic holes below instability threshold
- Conclusions and open questions

1. Satellite observations

Magnetic structures (**humps** or **holes**)
that are quasi-stationary in the plasma frame,
with **no or little change in the magnetic field direction** are commonly observed in the
solar wind and the planetary magnetosheaths.

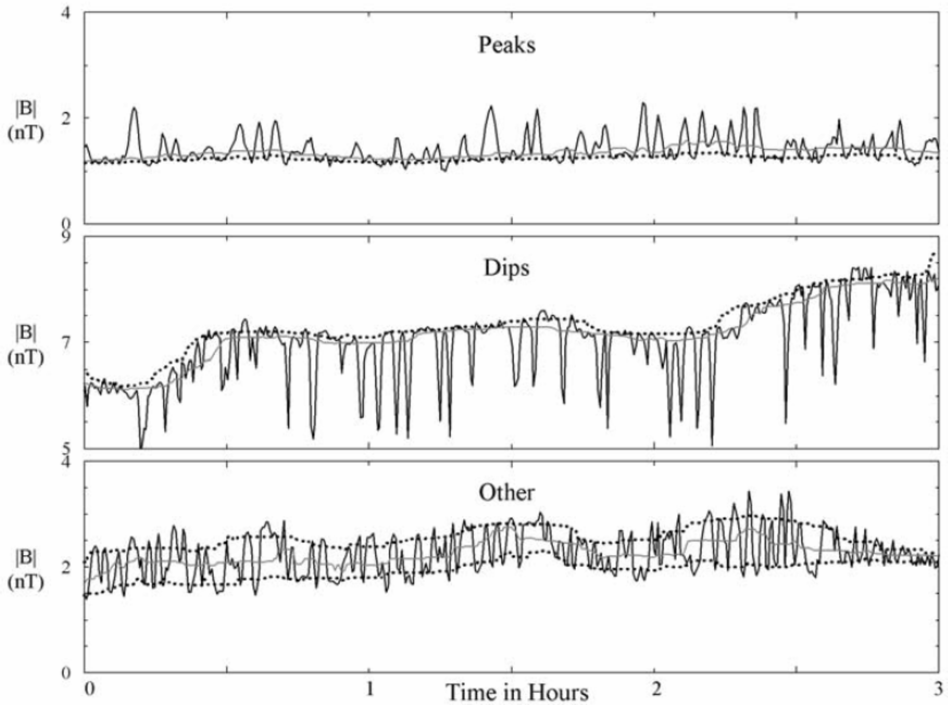

Figure 1. Each panel shows 3 hours of Galileo magnetometer field magnitude data (solid black line), appropriate quartiles (dotted), and the median value (solid gray) computed using 20 min sliding windows with single sample shifts. The panels show examples of "peaks" (top), "dips" (middle), and "other" (bottom) structures.

Joy et al. J. Geophys. Res. **111**, A12212 (2006)

Structures observed in the Jovian magnetosheath

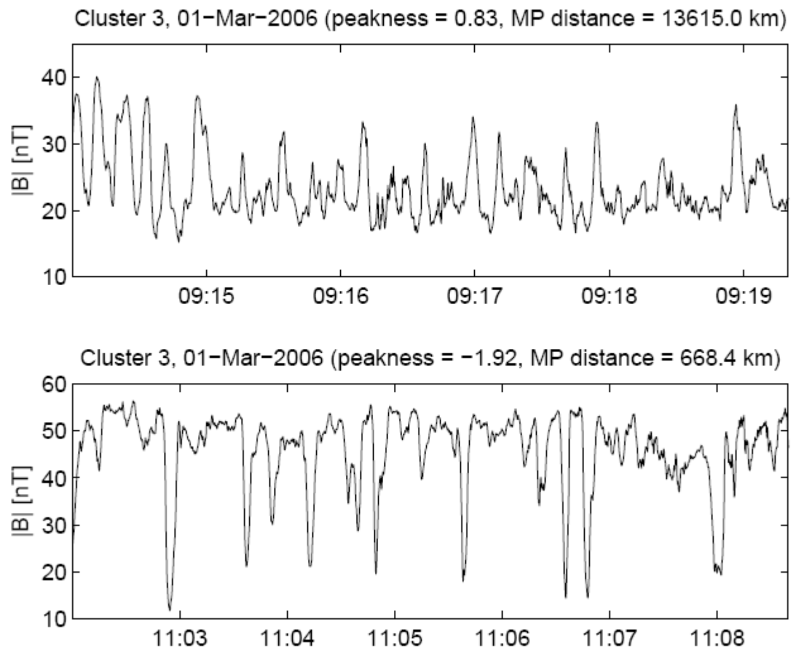

Figure 1. An example of mirror mode structures of the two types. Top panel: peaks (peakness = 0.83), bottom panel: dips (peakness = -1.92).

Soucek, Lucek & Dandouras JGR **113**, A04203 (2008)

Structures observed in
the terrestrial magnetosheath

Usually viewed as **nonlinear mirror modes**

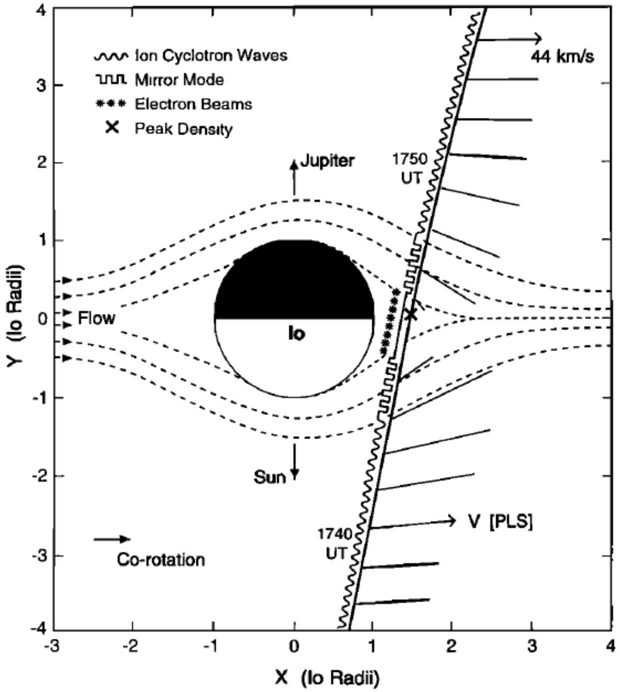

Figure 1. Overview of the Galileo-Io flyby geometry showing the locations of the mirror mode and ion cyclotron wave observations. (Figure adapted from *Russell et al.* [1997], and velocity vectors taken from *Frank et al.* [1996].)

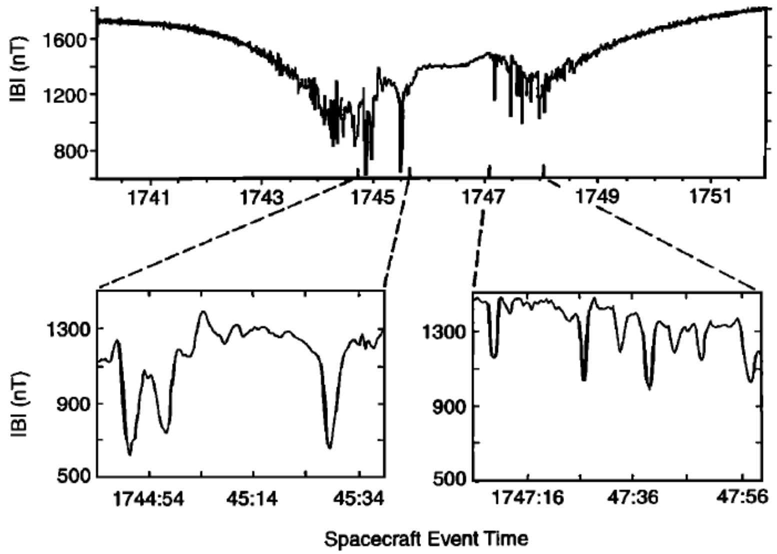

Figure 2. Magnetometer data from the Io flyby [*Kivelson et al*, 1996] in right-handed System III (1995) coordinates. The expanded panels show in detail the mirror-mode structures seen on the edges of the Io wake.

Mirror–mode structures in the wake of Io, as observed by Galileo

Russell et al., JGR **104** (A8) 17471 (1999)

Huddleston et al., JGR **104** (A8) 17479 (1999)

Mirror modes in Venus'magnetosheath

Volwerk et al., GRL **35**, L12204 (2008)
JGR **113**, E00B16 (2008)

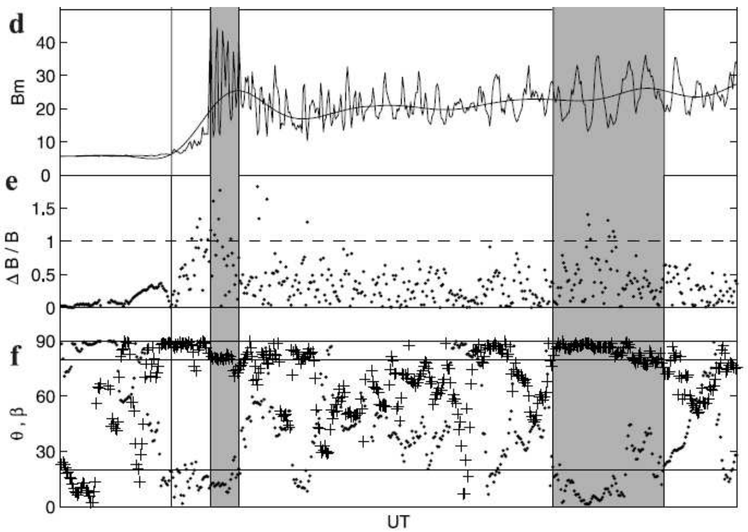

Figure 1. The magnetic field data for 5 May 2006. The spacecraft moves from the solar wind (SW), through the BS (BS) into the magnetosheath (MS). (e) and (f) The fluctuation of the magnetic field $\Delta B/B$ and the angle θ_{Bmv} between the maximum variance direction and the mean magnetic field (dots), and the angle β_{Bmv} between the minimum variance direction and the mean magnetic field (pluses).

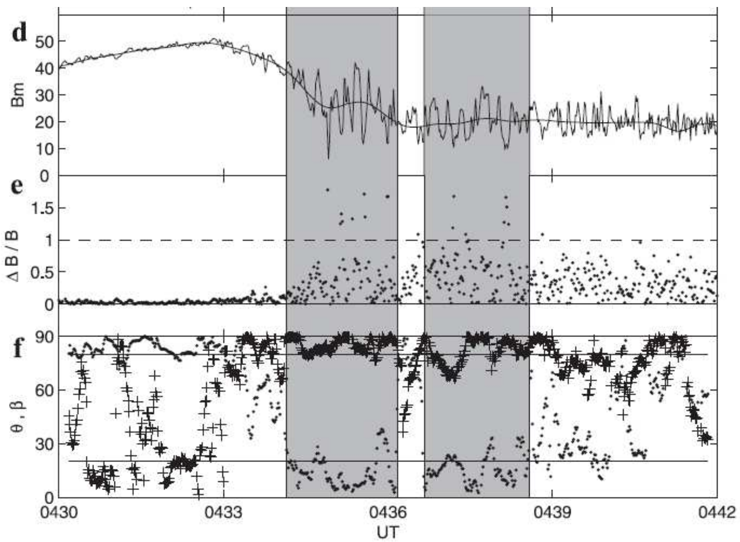

Figure 3. The magnetic field data for 2 October 2006. The spacecraft moves from periapsis in Venus' magnetosphere (MSp), through the magnetopause (MP) into the magnetosheath (MS). (e) and (f) The fluctuation of the magnetic field $\Delta B/B$; the angle θ_{Bmv} between the maximum variance direction and the mean magnetic field (dots), and the angle β_{Bmv} between the minimum variance direction and the mean magnetic field (pluses).

MM waves are identified as having large strengths $\Delta B/B$, and small angles θ_{Bmv} between the maximum variance and the magnetic field direction $\theta_{\mathrm{Bmv}} \leq 30^\circ$ [*Price et al.*, 1986].
(linear holes)

Conditions for peaks or dips

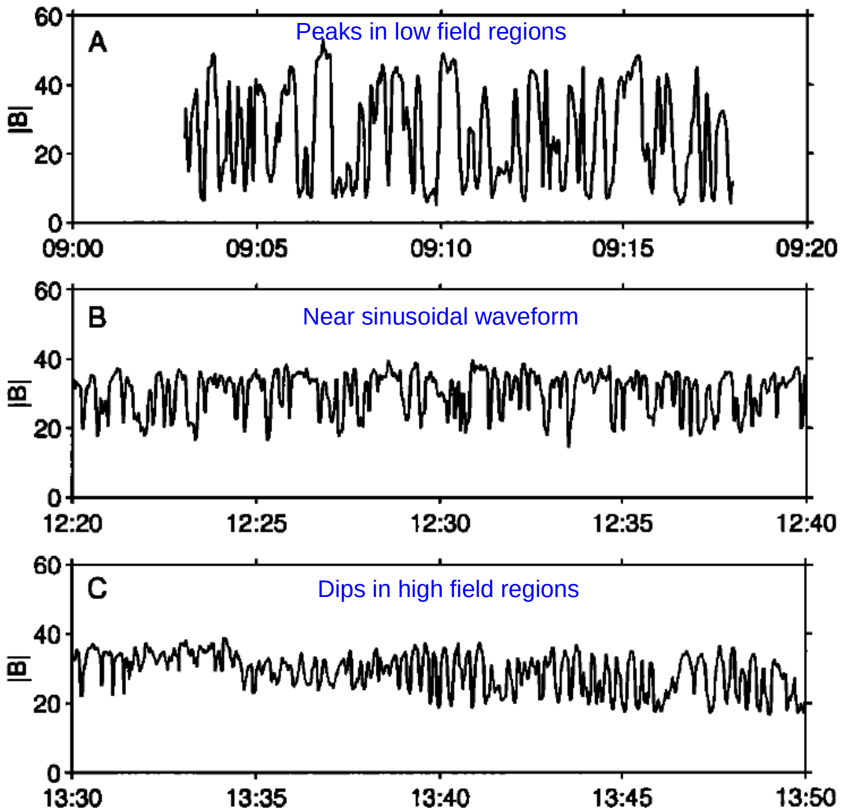

Figure 2. A, B and C show the field magnitude recorded during three intervals from 20 Dec 1997. They illustrate three forms of mirror structure: peaks, dips and a near sinusoidal waveform.

Lucek et al. GRL **26,** 2159 (1999)

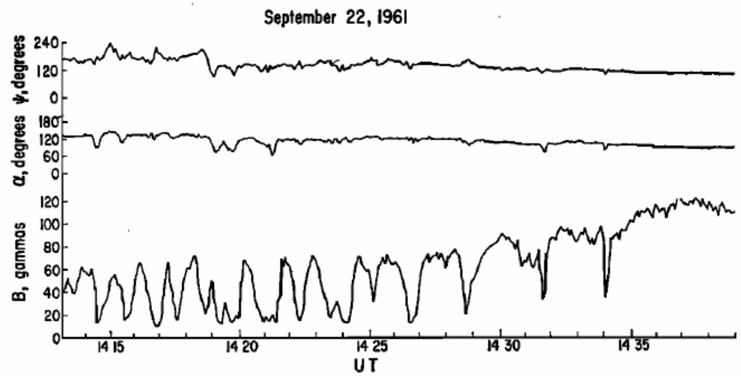

Fig. 1. Magnetic field magnitude B and direction angles α and ψ are presented in satellite coordinates for part of a highly disturbed orbit. The angle between the magnetic field and the satellite spin axis is α. The angle between the magnetic field and the sun, as projected onto the satellite's equatorial plane is ψ. Each point plotted represents the average of 16 individual field measurements taken during a 5-sec time interval.

Kaufmann et al., J. Geophys. Res. **75,** 4666 (1970)

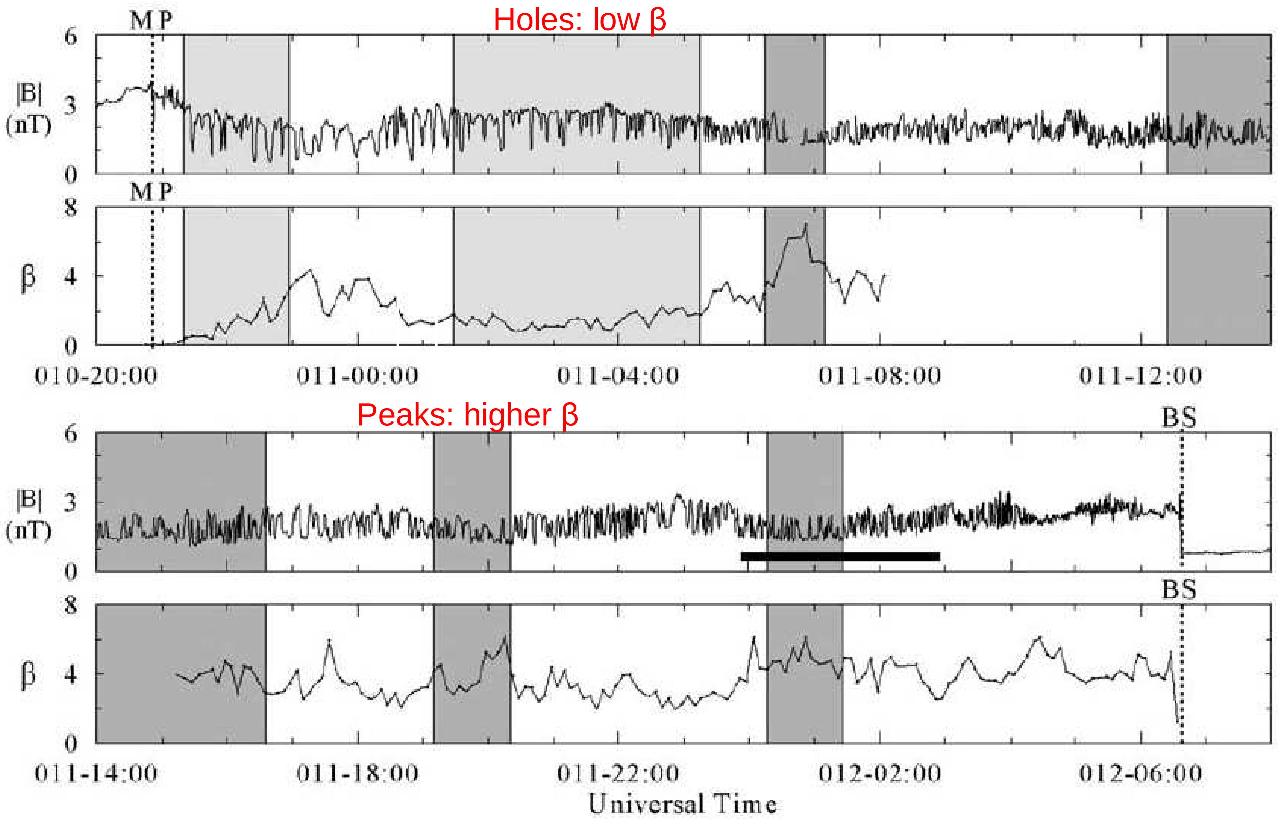

Figure 8. Galileo magnetic field and plasma β observations from the outbound pass of the 29th orbit. The shading convention used here is the same as in Figure 2. The heavy black line indicates an interval of amplitude saturation. The vertical dotted lines mark the bow shock and magnetopause crossing times.

Depending on local values of β, magnetic holes or humps are preferentially formed.

Same conclusion by Bavassano-Cattaneo et al. 1998 (Saturn's magnetosheath),
Soucek, Lucek & Dandouras 2008 (Earth's magnetosheath).

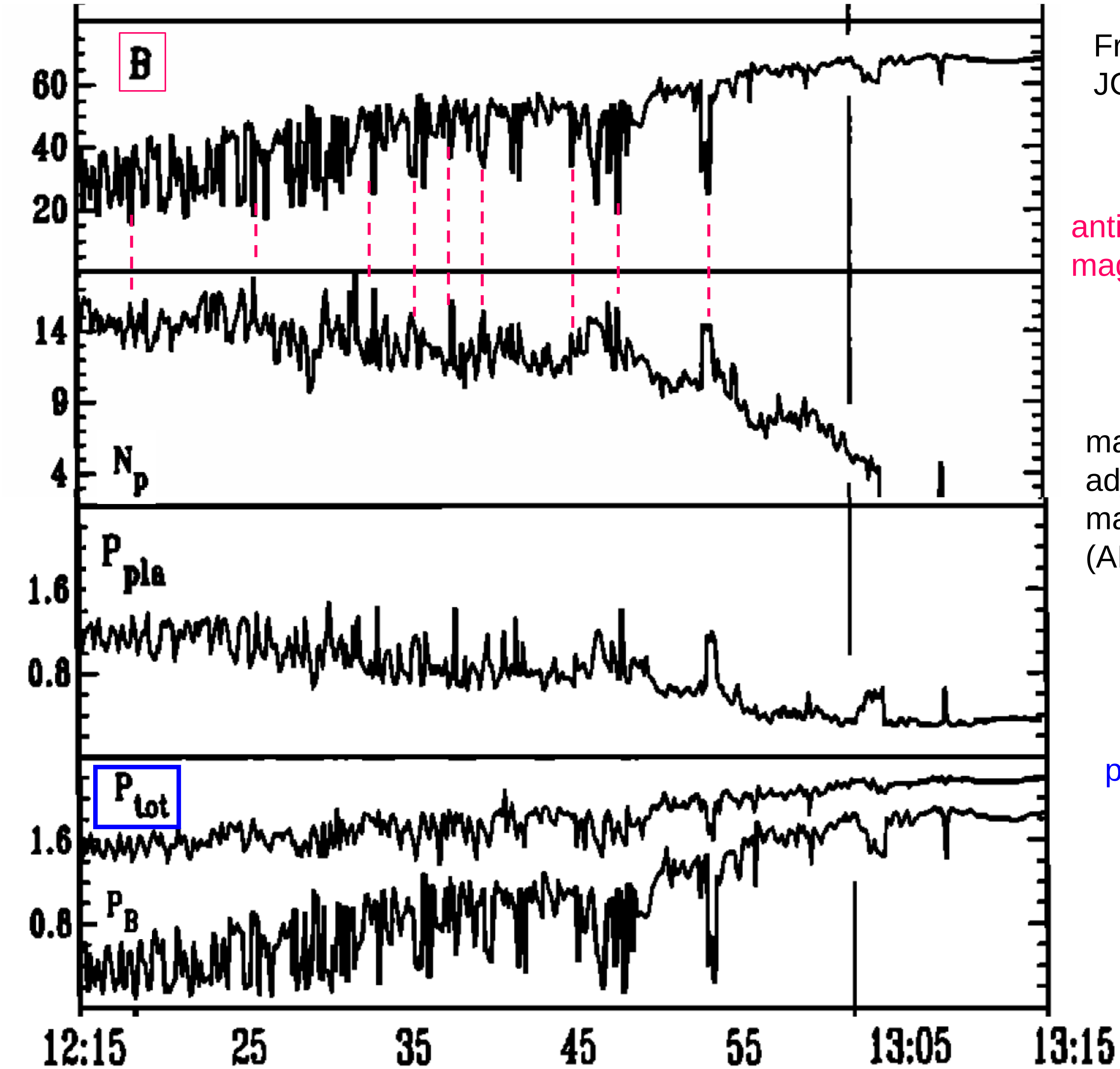

From Phan et al.
JGR 99, 121 (1994)

anticorrelation
magnetic field - density

magnetosheath region
adjacent to the dayside
magnetopause
(AMPTE/IRM satellite).

pressure equilibrium

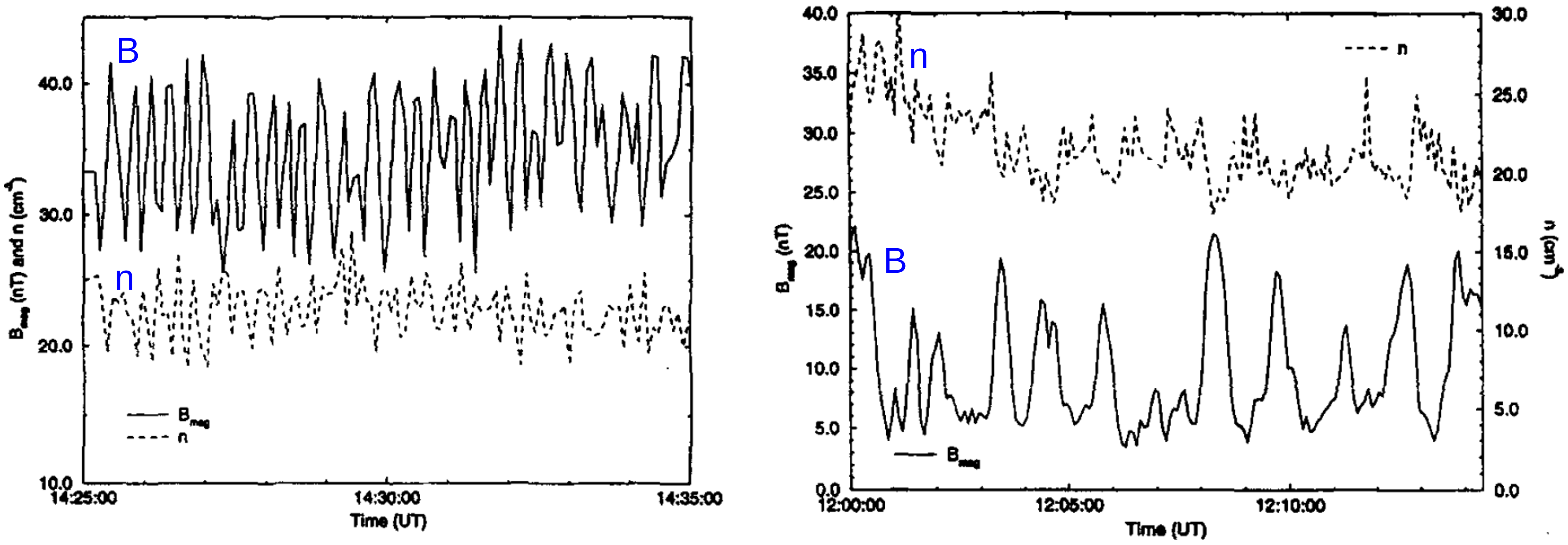

Strong anti-correllation of magnetic field and density for nearly sinusoidal (left) and peak (right) mirror modes.

Leckband et al., Adv. Space Res. **15**, 345 (1995)

Measurement by AMPTE-UKS satellite in the magnetosheath.

Magnetic holes may display different shapes (sharp or wide)

Free solar wind (Ulysses)

Jovian magnetosheath (Ulysses)

Free solar wind (Helios)

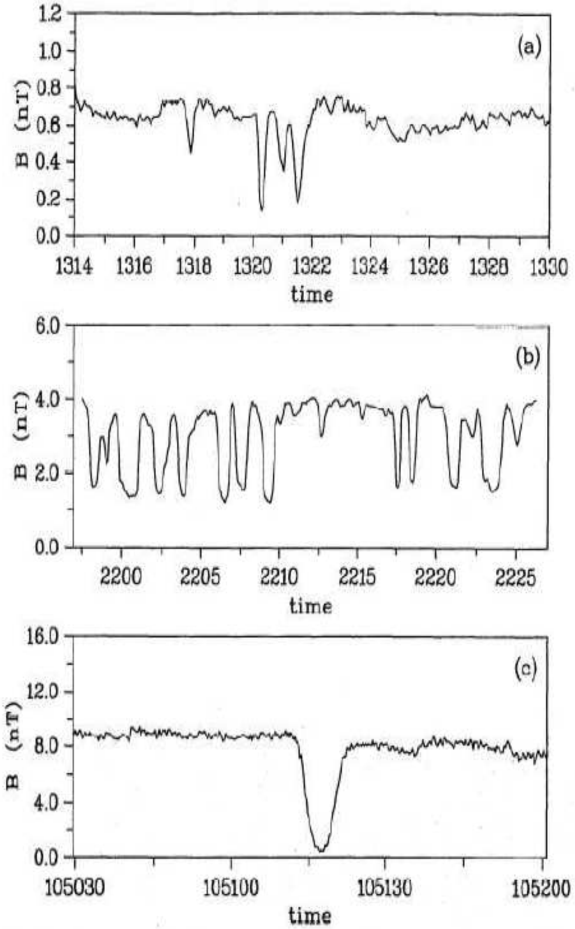

Figure 1. Examples of magnetic holes observed (a) by Ulysses in the free solar wind (taken from Figure 2 of *Winterhalter et al.* [1994], (b) by Ulysses in the magnetosheath of Jupiter, called mirror mode structures (from Figure 5 of *Erdös and Balogh* [1996]), and (c) by Helios in the free solar wind (data courtesy of K. Sperveslage and F.M. Neubauer, University of Köln, 1999). Shown is the magnetic field magnitude.

Baumgärtel JGR **104** (A12), 28295 (1999)

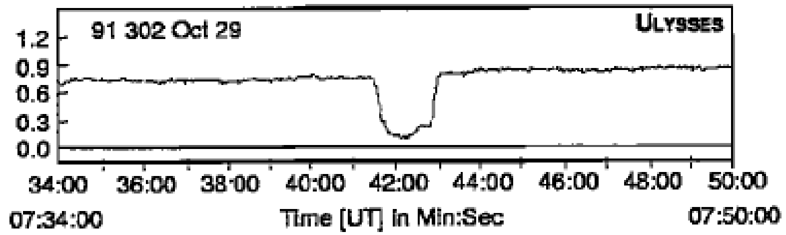

Winterhalter et al. (2000)

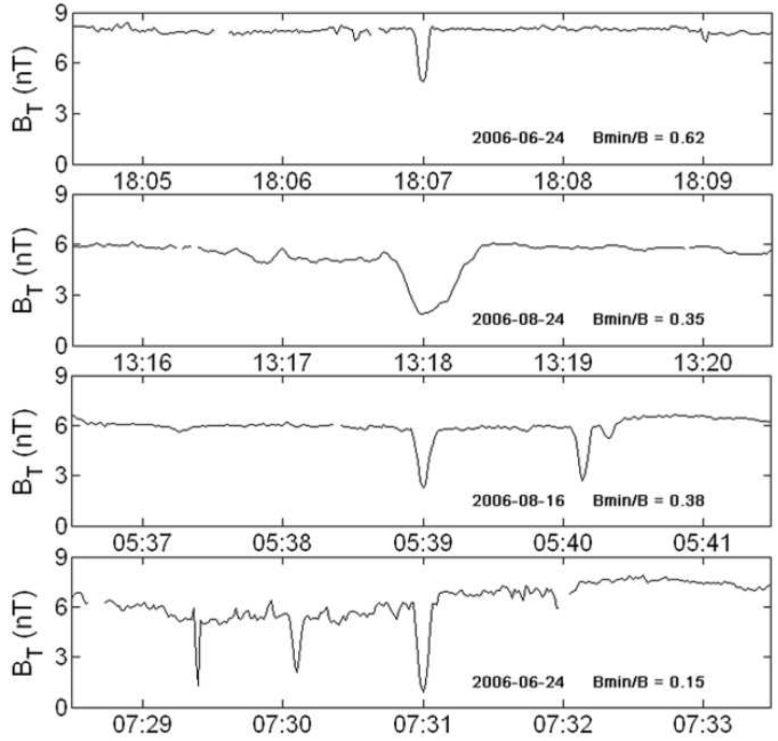

Figure 2. More examples of the mirror mode structures in the solar wind.

Zhang et al. GRL **35**, L10106 (2008)

Do these structures have a unique origin?

Other magnetic structures in the solar wind (Sperveslage et al. NPG 7, 191, 2000)

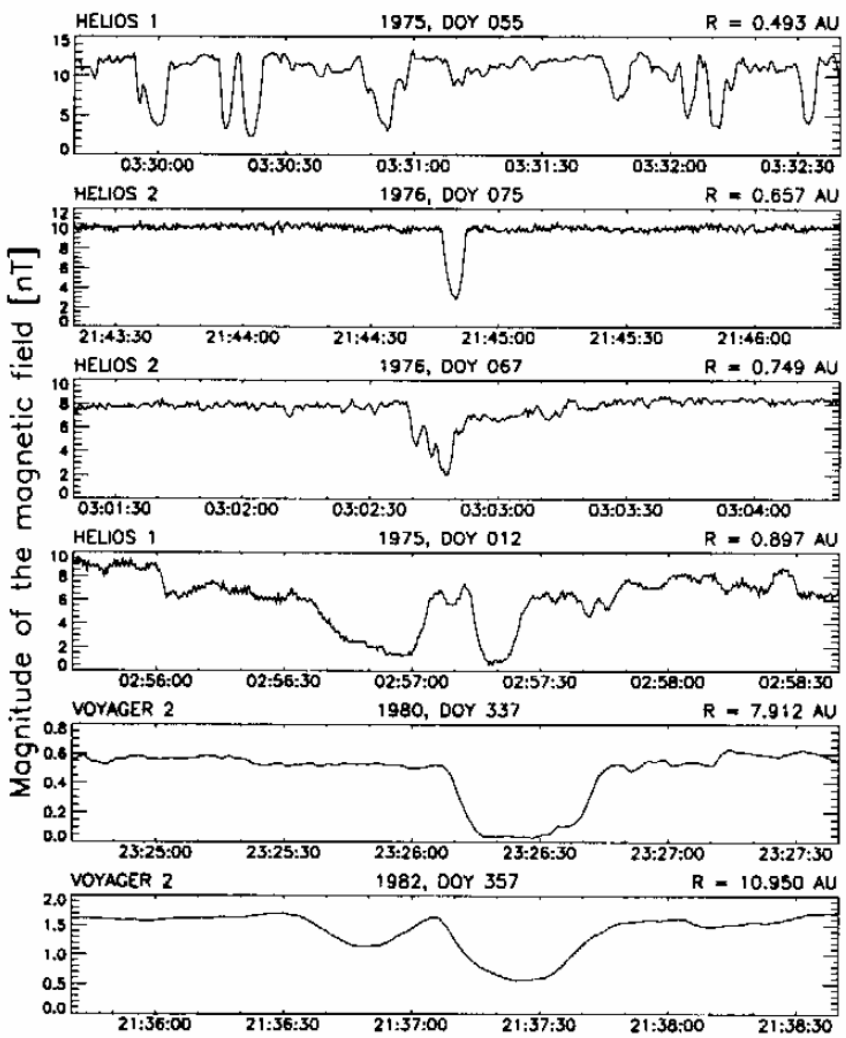

Fig. 2. Examples of magnetic holes in the highest resolution data of the missions Voyager 2 (1.92 s), Helios 1 and 2 (0.25 s); time intervals are three minutes.

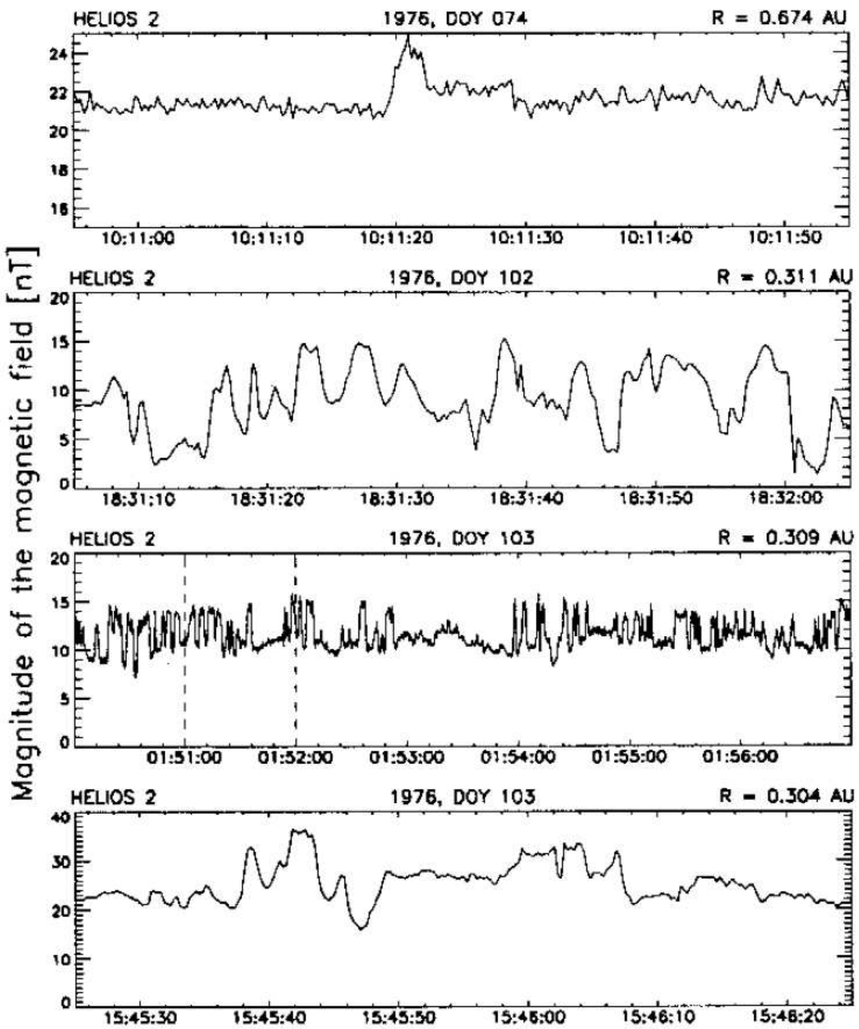

Fig. 3. Examples of magnetic enhancements in the highest resolution data of the mission Helios 2; time intervals are one minute except for panel 3.

Evidence of huge magnetic holes in the solar wind
(Stevens & Kasper, JGR **112,** A10905 (2007))

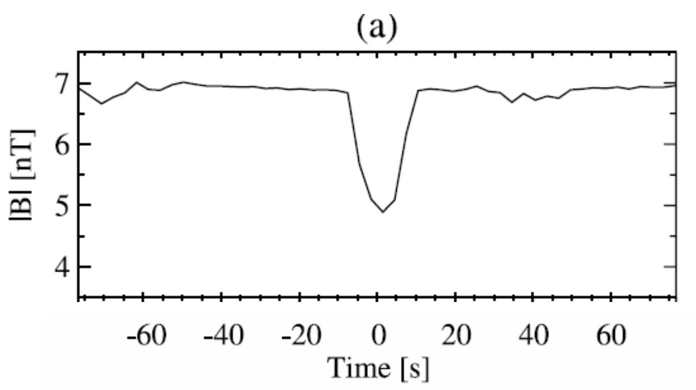

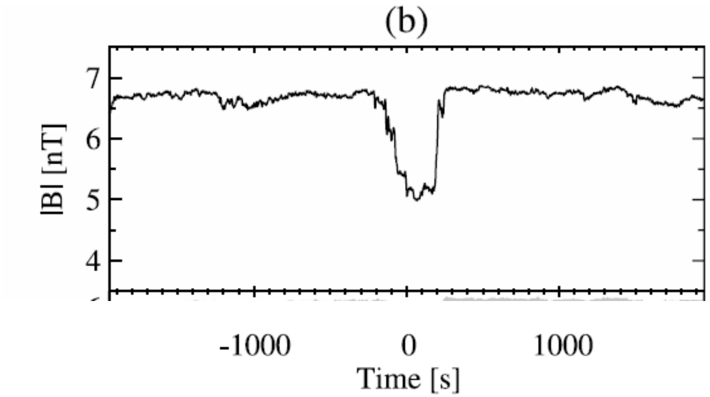

(a) This nagnetic hole has a cross-sectional width of about 100 proton gyroradii
(b) This hole, however, is about 4000 proton gyroradii across.

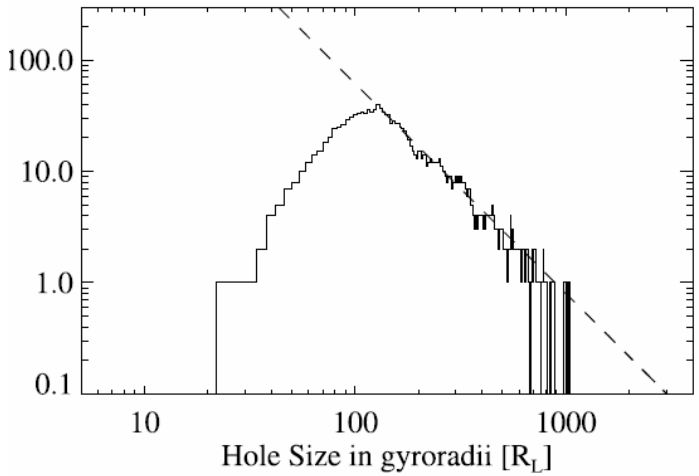

Effect of solar wind expansion on mirror modes?

Alternative origin :Alfvén waves propagating at large angle to the ambient magnetic field [Buti et al., JGR 2001]

Do kinetic effects play a role is so big structures ?

Main properties of observed structures:

- Structures are quasi-static in the plasma frame

•Small change in the magnetic field direction

- Observed in regions displaying: ion temperature anisotropy $T_{i\perp} > T_{i\,\|}$
  β of a few units
  (conditions met under the effect of plasma compression in front of the magnetopause).
  Not always in a mirror unstable regime.

- Magnetic fluctuations mostly affect the parallel component.

- Cigar-like structures, quasi-parallel to the ambient field, with a transverse scale of a few Larmor radii.

- Density is anticorrelated with magnetic field amplitude.

Origin of these structures is still not fully understood.

Usually viewed as nonlinearly saturated states of the mirror instability, or possibly, in particular in the solar wind, remnants of mirror structures created upstream of the point of observation (Winterhalter et al. 1995).

Other recent interpretations:

- trains of slow-mode magnetosonic solitons (Stasiewicz 2004)
- mirror instability is the trigger, generating high amplitude fluctuations that evolve such as to become nonlinear solutions of isotropic or anisotropic plasma equations (Baumgärtel, Sauer & Dubinin 2005)

Linear instability

cold electrons, $f = f(v_\parallel^2, v_\perp)$

Venedov and Sagdeev (1958), Chandrasekhar et al. (1958), Hasegawa (1969), Hall (1979), Gary (1992), McKean et al. (1992,1994), Southwood and Kivelson (1993), Pantellini & Schwartz 1995, Pokhotelov et al. (2005 and references therein), Hellinger (2007).

Instability condition: $\boxed{\Gamma = \beta_\Gamma - \beta_\perp - 1 > 0}$ (Shapiro & Shevchenko 1964)

$$\beta_\perp = \frac{mn}{p_B}\int \frac{v_\perp^2}{2} f d^3v \qquad \beta_\parallel = \frac{mn}{p_B}\int v_\parallel^2 f d^3v \qquad \beta_\Gamma = -\frac{mn}{p_B}\int \frac{v_\perp^4}{4}\frac{\partial f}{\partial v_\parallel^2} d^3v$$

n is the background density of the protons, m their mass

$p_B = B_0^2/8\pi$ background magnetic pressure

Linear growth rate (near threshold):

$$\boxed{\gamma_{\boldsymbol{k}} = \sqrt{\frac{2}{\pi}}|k_\parallel|\tilde{v}\left(\Gamma - \frac{3}{2}\tilde{r}^2 k_\perp^2 - \frac{k_\parallel^2}{k_\perp^2}\chi\right)}$$

$$\tilde{v}^{-1} = -\sqrt{2\pi}\frac{mn}{p_B}\int \frac{v_\perp^4}{4}\delta(v_\parallel)\frac{\partial f}{\partial v_\parallel^2} d^3v$$

$$\chi = 1 + \frac{1}{2}(\beta_\perp - \beta_\parallel)$$

$$\tilde{r}^2 = -\frac{mn}{24 p_B}\frac{1}{\Omega^2}\int \left(v_\perp^6 \frac{\partial f}{\partial v_\parallel^2} + 3v_\perp^4 f\right) d^3v$$

For a bi-Maxwellian distribution:

$$\beta_\perp = mnv_{th\perp}^2/p_B$$
$$\beta_\parallel = mnv_{th\parallel}^2/p_B$$
$$\tilde{v} = v_{th\parallel}/\beta_\Gamma$$
$$\beta_\Gamma = \beta_\perp^2/\beta_\parallel$$
$$\tilde{r} = v_{th\perp}(\beta_\Gamma - \beta_\perp)^{1/2}/\Omega$$

Instability condition:

$$\boxed{\Gamma^* \equiv \beta_\perp\left(\frac{\beta_\perp}{\beta_\parallel} - 1\right) - 1 > 0}$$

Growth rate:

$$\gamma_{\boldsymbol{k}} = |k_z| v_{\text{th}\parallel}\frac{\beta_\parallel}{\sqrt{\pi}\beta_\perp}\left[\frac{\beta_\perp}{\beta_\parallel} - 1 - \frac{1}{\beta_\perp} - \frac{k_z^2}{k_\perp^2\beta_\perp}\left(1 + \frac{\beta_\perp - \beta_\parallel}{2}\right) - \frac{3}{4\beta_\perp}k_\perp^2\rho_L^2\right]$$

(ρ_L: ion Larmor radius)

Linear mirror instability (continued)

- Zero-frequency instability.

- Driven by Landau wave-particle resonance and quenched at small-scales by finite Larmor radius effects.

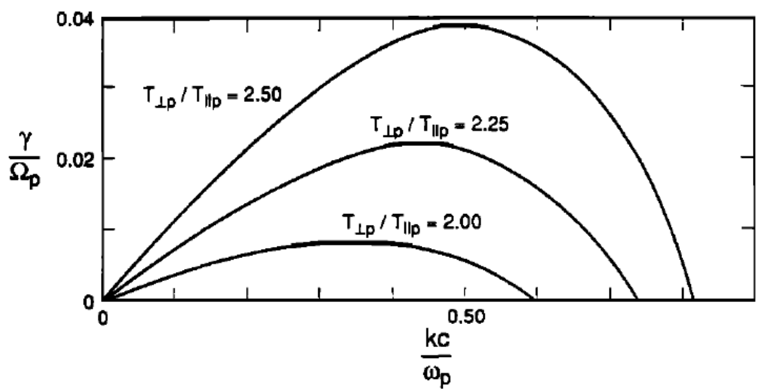

Fig. 2. The growth rate of the mirror instability as a function of wavenumber at three different values of the proton temperature anisotropy. Here and in the following figures (unless stated otherwise) the other plasma parameters are $\beta_p = 1.00$, $m_p/m_e = 1836$, $T_e/T_{\|p} = 1.00$, and $v_A/c = 1.0 \times 10^{-4}$. For each curve the angle of propagation corresponds to the maximum growth rate at that value of the anisotropy: at $T_{\perp p}/T_{\|p} = 2.00$, $\theta = 71°$; at $T_{\perp p}/T_{\|p} = 2.25$, $\theta = 66°$; and at $T_{\perp p}/T_{\|p} = 2.50$, $\theta = 63°$.

Gary, JGR **97** (A6), 8519 (1992).

See also Hall, *J. Plasma Phys.* ***21****, 431 (1979).*

- At least near threshold, it develops at large angle with respect to the ambient field.
At small or moderate angle and/or smaller β, Ion Cyclotron Anisotropic Instability can be dominant.
Nevertheless, numerical simulations suggest that mirror modes could dominate in the nonlinear regime *("Competition between the mirror-mode instability and the L-mode electromagnetic ion cyclotron instability: results from comparison of 2-D and 3-D simulations"*Shoji,Omura,Tsurutani,Verkhoglyadova http://rp.iszf.irk.ru/hawk/URSI2008/paper/HP04p3.pdf)

Understanding of the nonlinear dynamics is still incomplete.

Magnetic holes are also observed in conditions for which the plasma is linearly stable (BISTABILITY).

$$\frac{T_\perp}{T_\parallel} - 1 > \frac{1}{\beta_\perp}$$

(instability condition for bi-Maxwellian distribution)

Skewness of magnetic fluctuations:
- when negative: magnetic holes
- when positive: magnetic humps

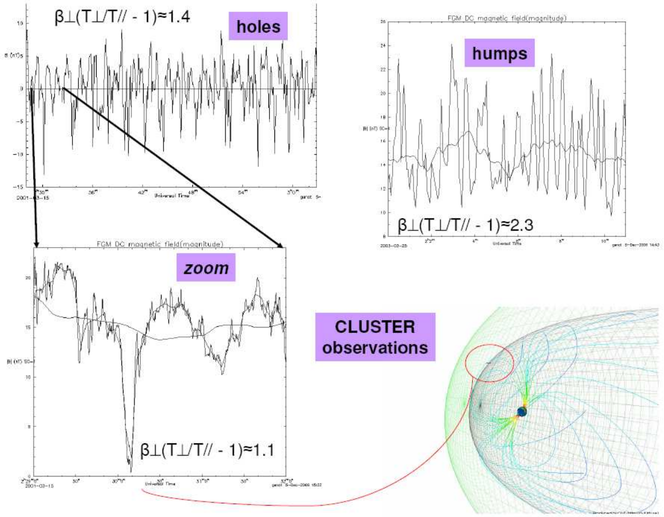

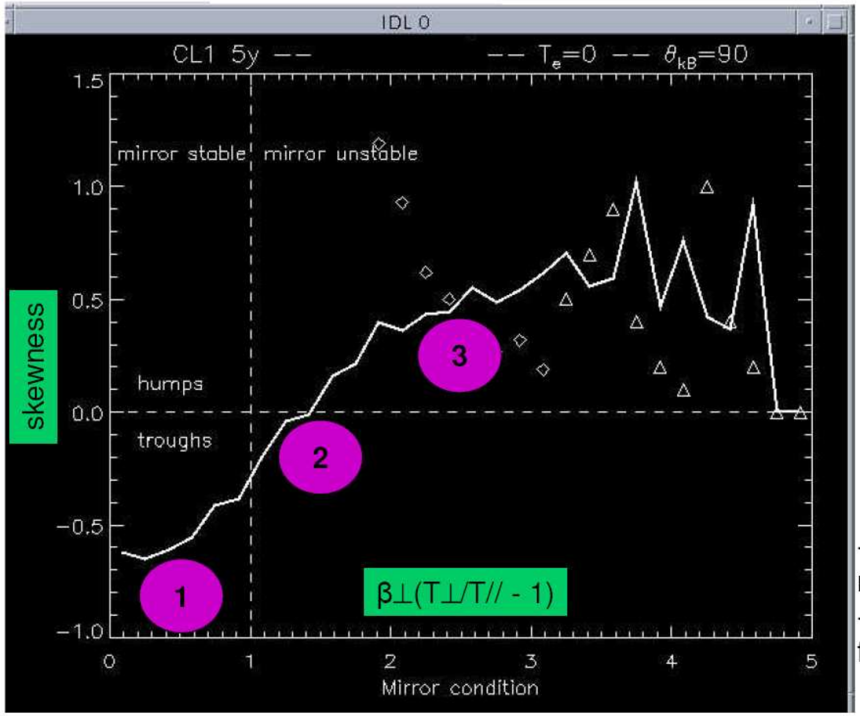

Distance to threshold

1
- Holes in small beta region
- Linearly stable or close to threshold
- *Bistability* region

2
- Linear mirror mode
- Classical sinusoidal shape

3
- Humps in large or moderate beta region
- Corresponds to the first phase of simulations

Magnetosheath CLUSTER data (Génot et al., AGU 2006)

Soucek, Lucek & Dandouras (JGR 2008): "peaks are typically observed in an unstable plasma, while mirror structures observed deep within the stable region appear almost exclusively as dips".

Bistability also observed in Jovian magnetosheath (Erdös and Balogh 1996)

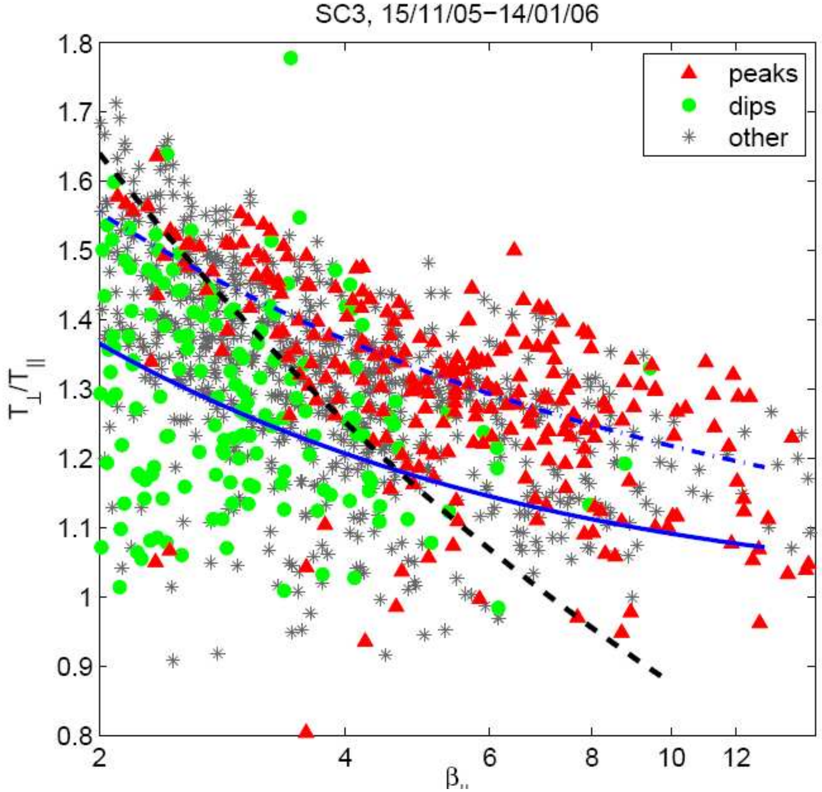

Figure 3. Distribution of mirror modes of different types in the anisotropy-beta plane. Red triangles denote peaks with $\mathcal{P} > 0.3$, green squares dips ($\mathcal{P} < -0.6$) and the remaining ambiguous mirror mode events are marked by grey stars.

Soucek, Lucek & Dandouras, JGR **113**, A04203 (2008)

Solid blue line: theoretical (bi-Maxwellian) mirror threshold

$$\frac{T_\perp}{T_{||}} > 1 + 1/\beta_\perp$$

Dashed-dotted blue line: empirical marginal stability

$$\frac{T_\perp}{T_{\|}} = 1 + \frac{a}{\beta_{\|}^{b}} \qquad a = 0.83 \quad b = 0.58$$

Black dashed line: fitted boundary between peaks and dips

$$\frac{T_\perp}{T_{||}} = \frac{2.15}{\beta_{||}^{0.39}}$$

Solar wind: "Although the plasma surrounding the holes was generally stable against the mirror instability, there are indications that the *holes may have been remnants of mirror mode structures* created upstream of the points of observation" (Winterhalter et al. 1995).

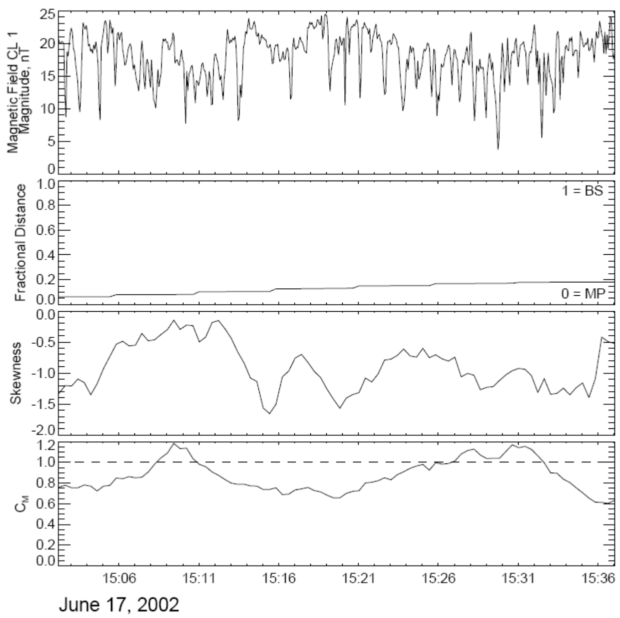

Observations of magnetic holes by Cluster 1 on June, 17^{th} 2002

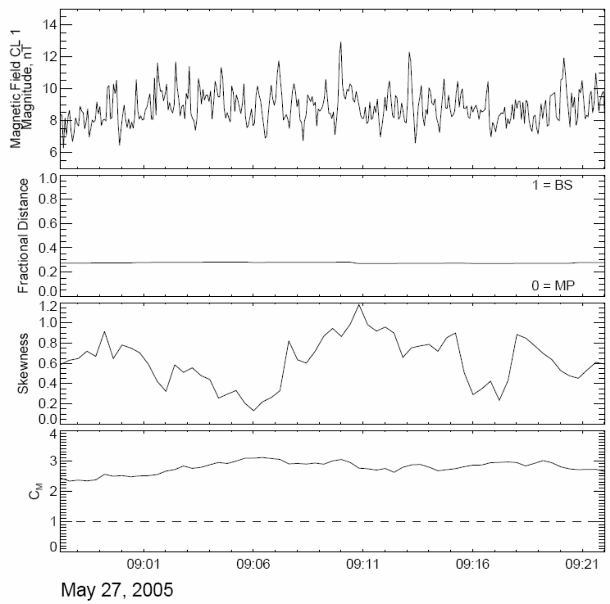

Observations of magnetic peaks by Cluster 1 on May, 27^{th} 2005

C_M <1 : subcritical
C_M >1 : supercritical
(for bi-Maxwellian equilibrium)

Magnetic holes: mostly in subcritical regime

Magnetic humps: in supercritical regime

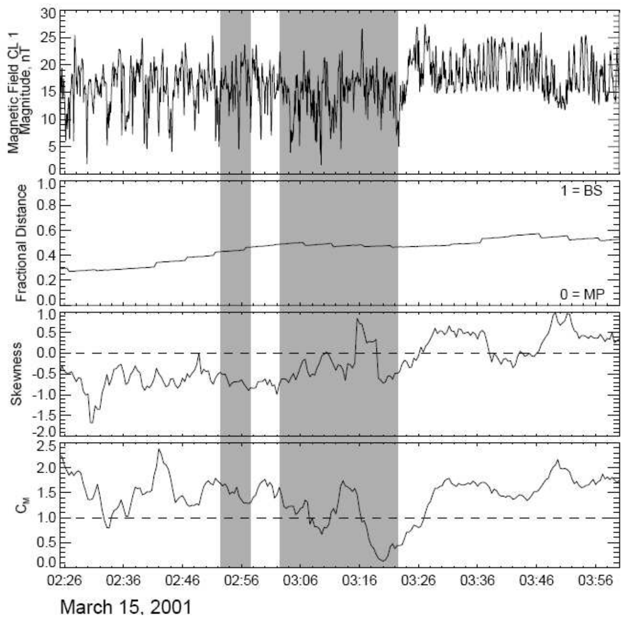

Observations of mirror structures by Cluster 1 on 15 March 2001.

Génot et al., Ann. Geophys. **27,** 601 (2009).

2. Numerical simulations of the Vlasov-Maxwell equations

Shed light on the time evolution and on the origin of the structures.

Mirror unstable regime near threshold in a large domain

1D simulation: $\theta_{kB} = 72.8^\circ$ (most unstable direction)

$\beta_{p\|} = 1 \; \beta_{p\perp} = 1.857 \quad \beta_e = 10^{-2}$

With a PIC code in a large domain:
Domain size= 2048 c/ωpi
Growth rate: 0.005 Ωp
1024 cells with 500 000 particles/cell

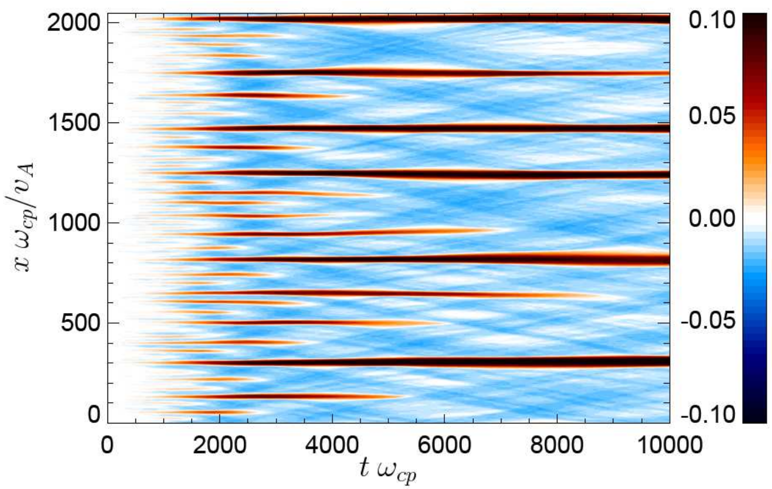

Color plot of the fluctuations of the magnetic field component B_η perpendicular to the direction ζ of spatial variation, as a function of ζ and t.

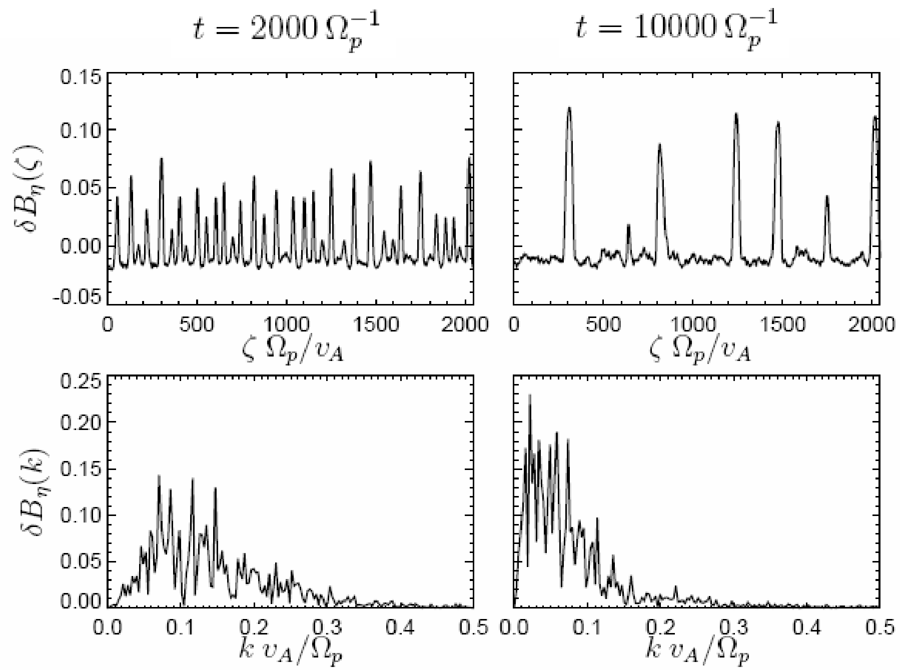

A large number of modes are excited.
Humps form and undergo coarsening.

QUESTION: What are the saturation mechanisms of the linear instability?

First mechanism suggested for saturation: based on **quasi-linear theory**
(Shapiro & Shevchenko 1963)

- Assumes space homogeneity
(thus absence of coherent structures).

- Can consequently be valid at early times only.

- Requires many modes in interaction, thus an extended domain.

- Mainly associated with a diffusion process in velocity space
  (dominantly along the ambient field).

Quasi-linear theory

(Shapiro & Shevchenko 1964)

$$\frac{\partial f}{\partial t} = \frac{\partial}{\partial v_\parallel} D_{\parallel\parallel} \frac{\partial f}{\partial v_\parallel} + \frac{1}{v_\perp}\frac{\partial}{\partial v_\perp} v_\perp \left(D_{\perp\parallel}\frac{\partial f}{\partial v_\parallel} + D_{\perp\perp}\frac{\partial f}{\partial v_\perp}\right)$$

f : velocity distribution function averaged over the space variables

$$D_{\parallel\parallel} = v_\perp^4 \sum_{\boldsymbol{k}} \frac{|b_{\boldsymbol{k}}|^2}{4} \frac{\gamma_{\boldsymbol{k}} k_\parallel^2}{k_\parallel^2 v_\parallel^2 + \gamma_{\boldsymbol{k}}^2}$$

$$D_{\perp\parallel} = -2\frac{v_\parallel}{v_\perp} D_{\parallel\parallel}$$

$$D_{\perp\perp} = v_\perp^2 \sum_{\boldsymbol{k}} \gamma_{\boldsymbol{k}} \frac{|b_{\boldsymbol{k}}|^2}{4}$$

$$b_{\boldsymbol{k}} = \delta B_z(\boldsymbol{k})/B_0$$

$$\frac{\partial b_{\boldsymbol{k}}}{\partial t} = \gamma_{\boldsymbol{k}} b_{\boldsymbol{k}}$$

linear growth rate

(Shapiro & Shevchenko 1964)

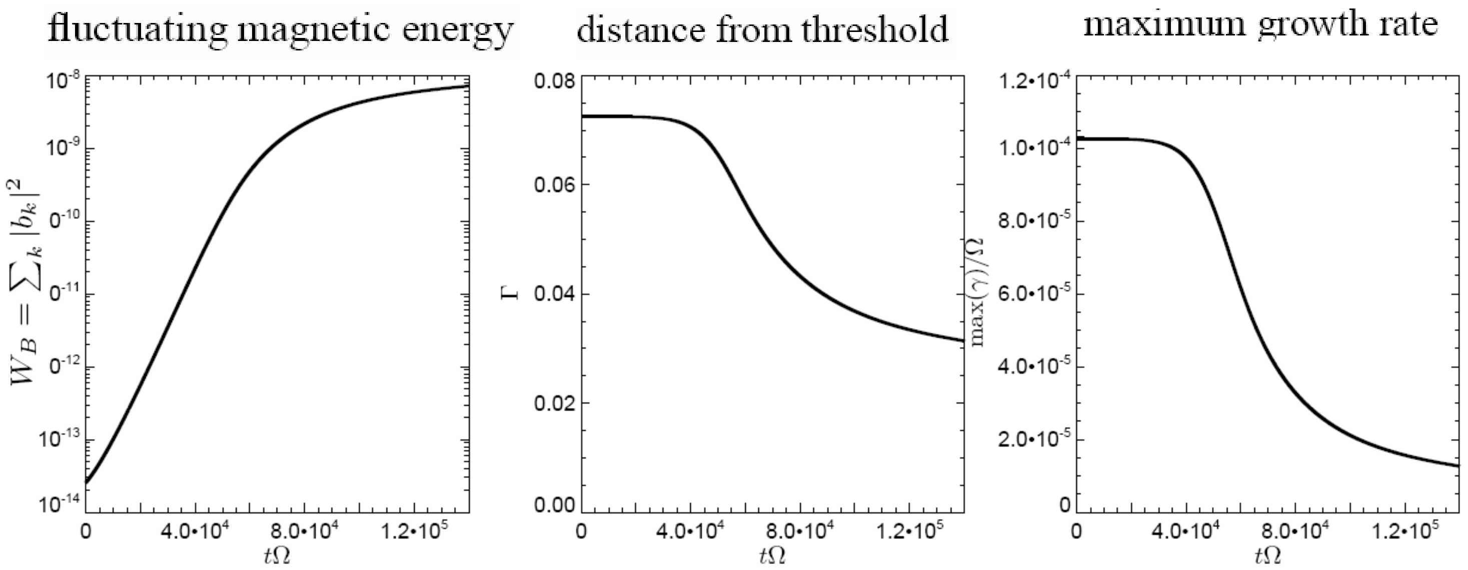

(Hellinger & al., GRL, submitted)

Perturbation of the space-averaged distribution function $\Delta f = f - f^{(0)}$

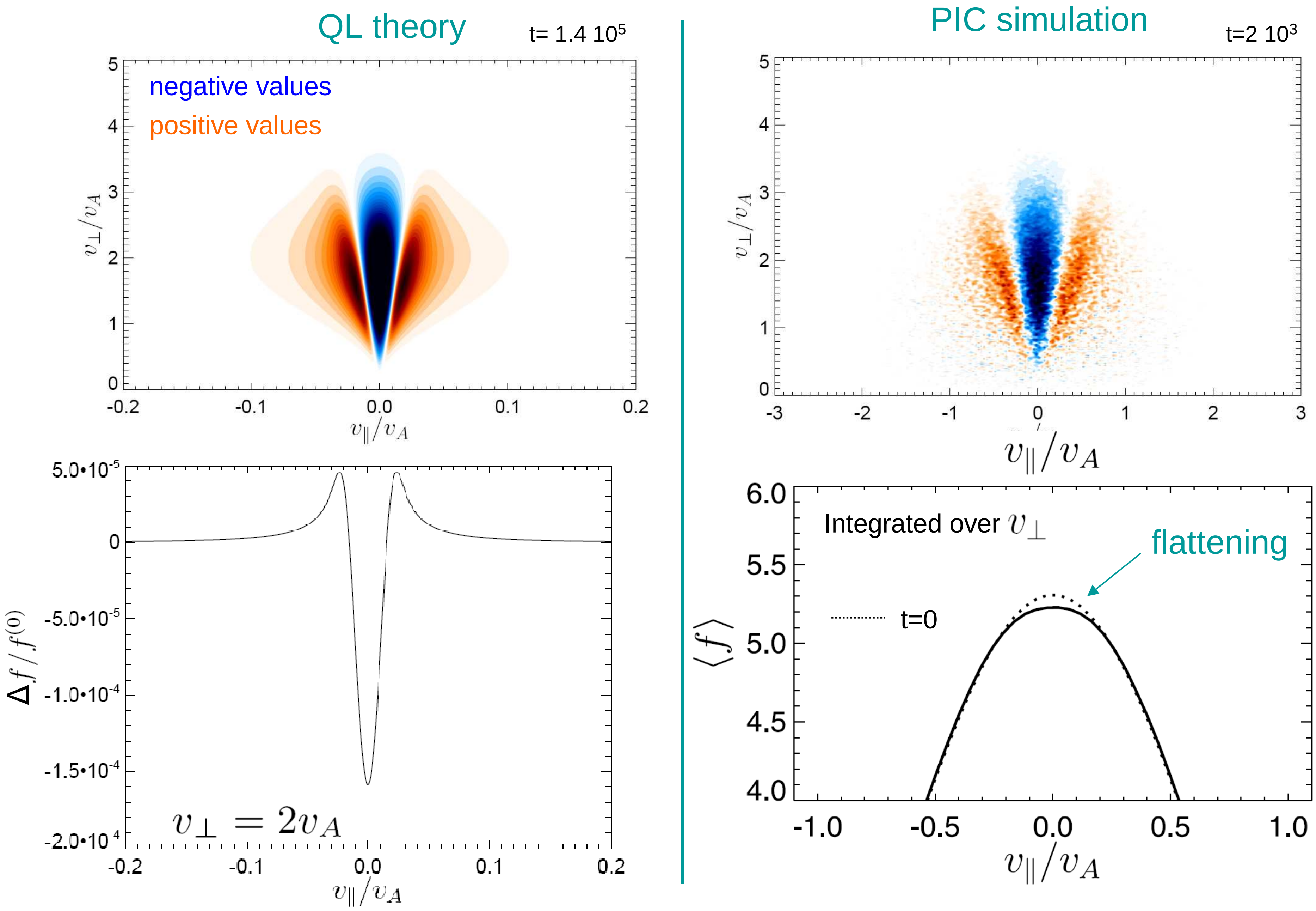

Quasi-linear theory cannot describe structure formation.

It traces the spatially independent part of the distribution function, while nonlinearities describing space variation (wave-wave interactions) are ignored.

Alternative theory: saturation of mirror modes by relaxation to locally marginal stability

(Kivelson and Southwood 1996, Pantellini 1998).

Phenomenological model where particles are divided in two groups that respond differently to the changing field.

Trapped particles with large pitch angle
Passing particles with small pitch angle $\alpha = \tan^{-1}(v_\perp / v_\parallel)$

In the rising field regions, trapped particles are excluded by the mirror force, leading to a decrease of the particle pressure (reduction of $\beta_\perp$) and evolution to marginal stability (with not important change in the particle energy).

In the well regions, no particle can be excluded.
Some trapped particles are cooled by loosing perpendicular energy (reduction of the temperature anisotropy).
Large reductions in the field are required in the wells in order to cool the trapped population enough to stabilize the system.

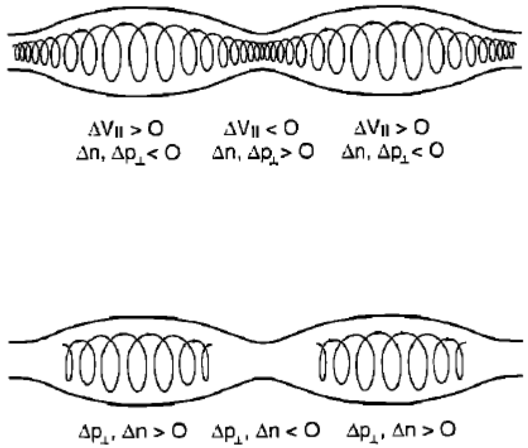

Figure 1. A schematic illustration of the distinction between the orbits of untrapped (upper panel) and trapped (lower panel) particles in a mirror geometry. Local velocity, density, and perpendicular pressure perturbations for adiabatic responses are characterized below each panel.

This model mostly predicts deep magnetic fields in conditions of marginal stability.
It hardly explains the formation of magnetic humps and does not address the phenomenon of bistability.

PIC simulation in an extended domain near threshold

Magnetic energy fluctuations

Gray scale plot of the magnetic fluctuations as a function of space and time.

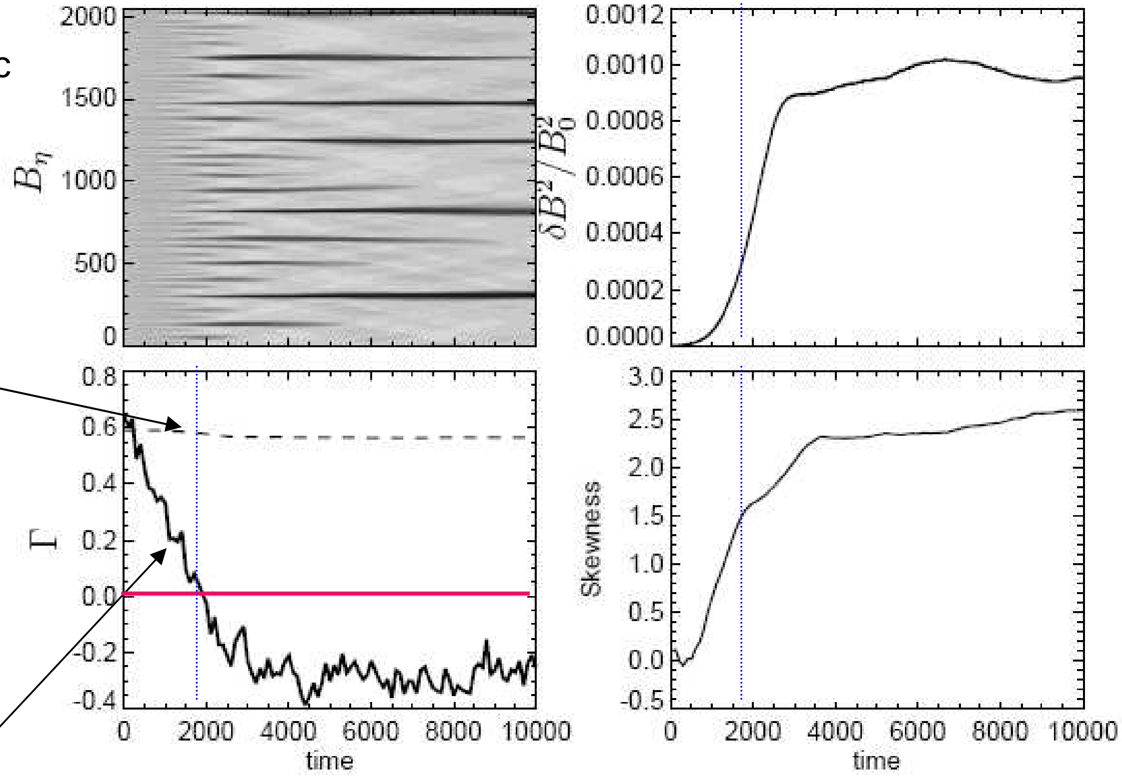

Bi-Maxwellian distance to threshold:

$$\Gamma^* = \beta_\perp \left(\frac{T_\perp}{T_\|} - 1 \right) - 1$$

Instantaneous distance to threshold:

$$\Gamma = -\frac{m}{p_B} \int \frac{v_\perp^4}{4} \frac{\partial f}{\partial v_\|^2} d^3v - \beta_\perp - 1$$

Instantaneous distance to threshold reaches negative values, a signature that quasi-linear theory ceases to apply when coherent structures begin to form.

The instability continues to take place while $\Gamma < 0$, due to hydrodynamic-type nonlinear effects.

Positive skewness: magnetic humps.

No relaxation to marginal stability regime

PIC hybrid simulations at moderate β

(Baumgärtel, Sauer & Dubinin, GRL, 2003)

Moderate distance from threshold

Initial random noise in a mirror instable regime leads to the formation of magnetic humps whose number decreases as time elapses.

Magnetic humps form and undergo coarsening.

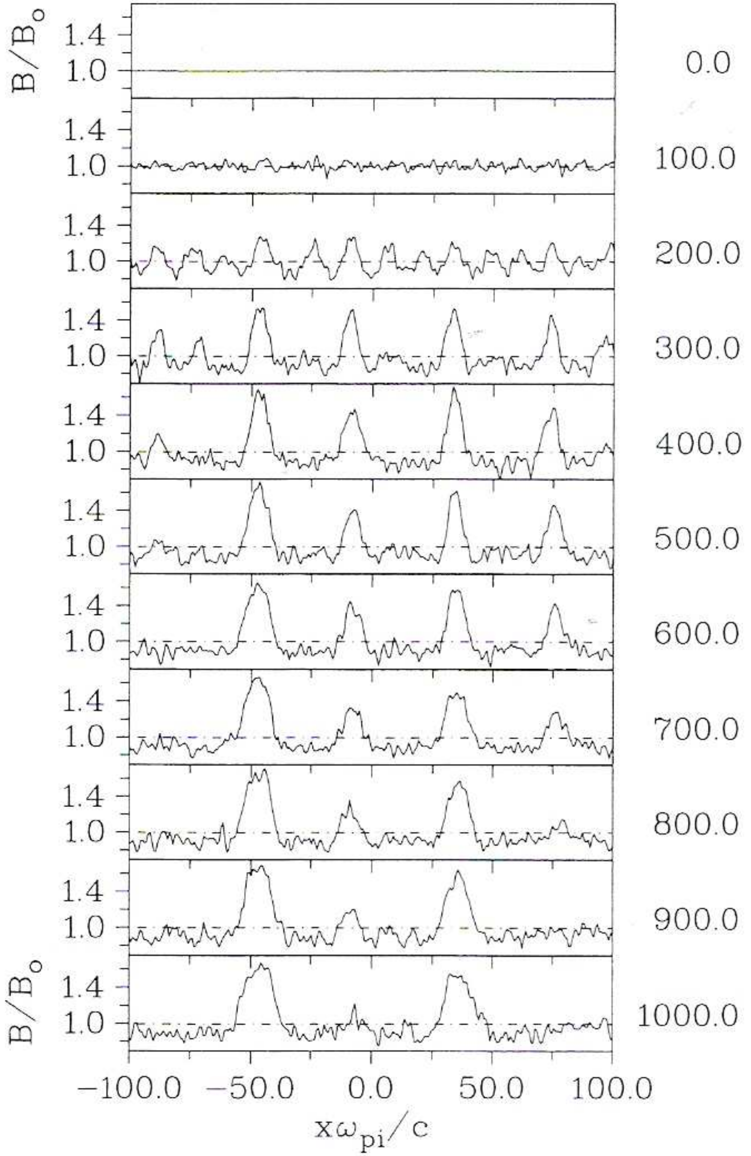

Figure 4. Space-time evolution of the magnetic field in an uniform, collisionless, anisotropic, mirror-unstable plasma with bi-Maxwellian proton distribution ($\beta_{i\perp} = 5$, $\beta_{i\|} = 2.5$, $\beta_e = 1$, $\theta = 80°$.

PIC simulation in a **small** computational domain

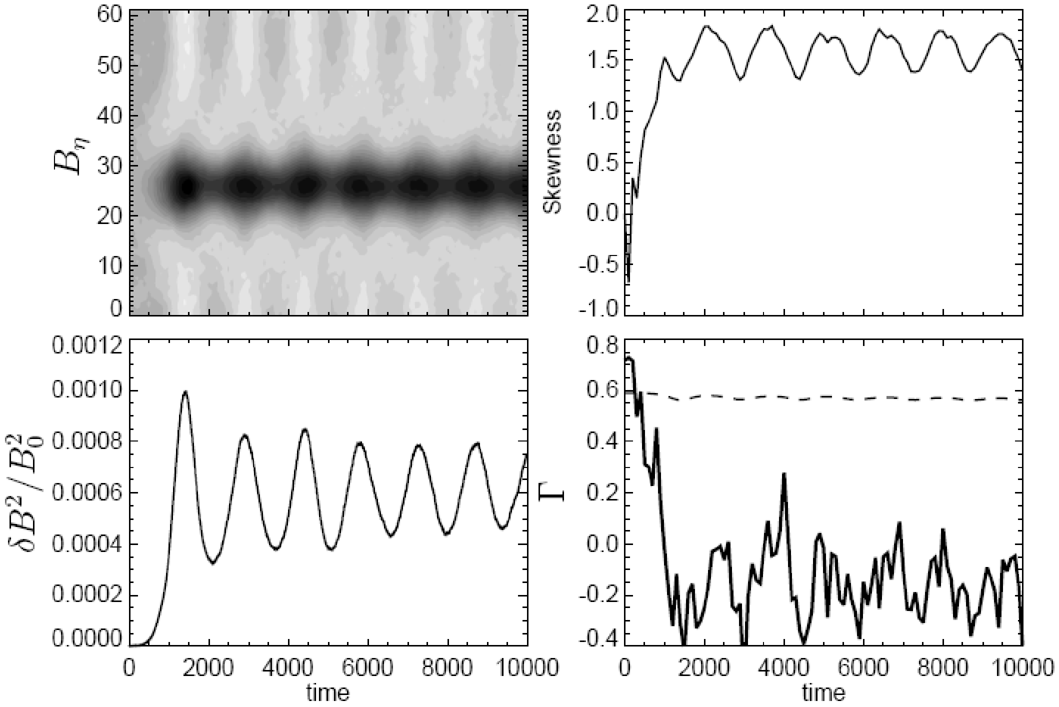

Oscillations of the magnetic energy fluctuations with a period consistent with the ion bounce time

$$\omega_{\rm tr}^2 = (1/2)v_{th_\perp}^2 k_{||}^2(\delta B/B_0)$$

Suggests that particle trapping is at the origin of oscillations.

.

Saturation by particle trapping in **gyrokinetic simulations** starting with a single mirror mode

(Qu, Lin & Chen, GRL **35**, L10108, 2008) PIC algorithm

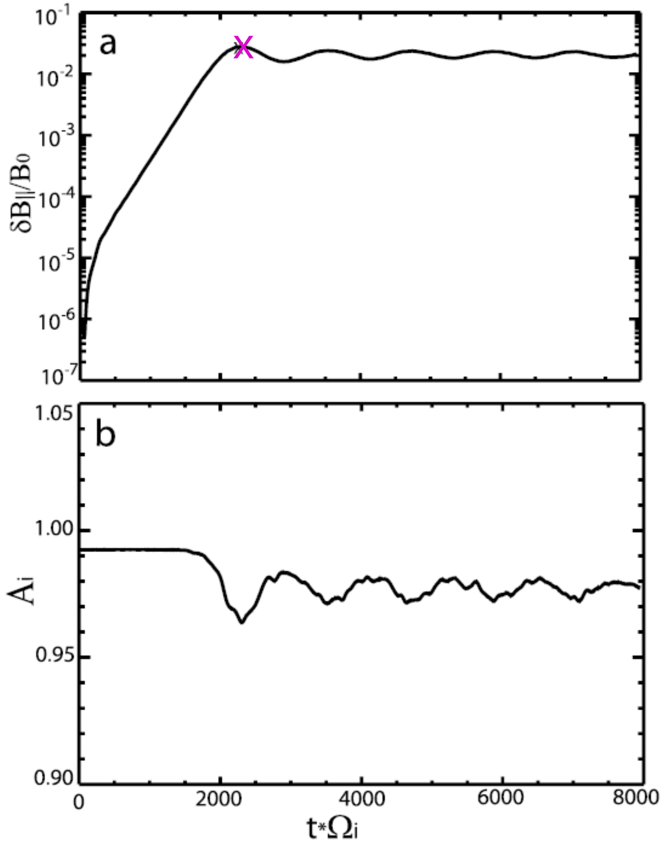

Figure 1. Time history of the amplitude of (a) the perturbed parallel magnetic field and (b) the ion temperature anisotropy for $\beta_{i,\perp} = 2$ and $A_i = 1$.

Anisotropy only weakly reduced

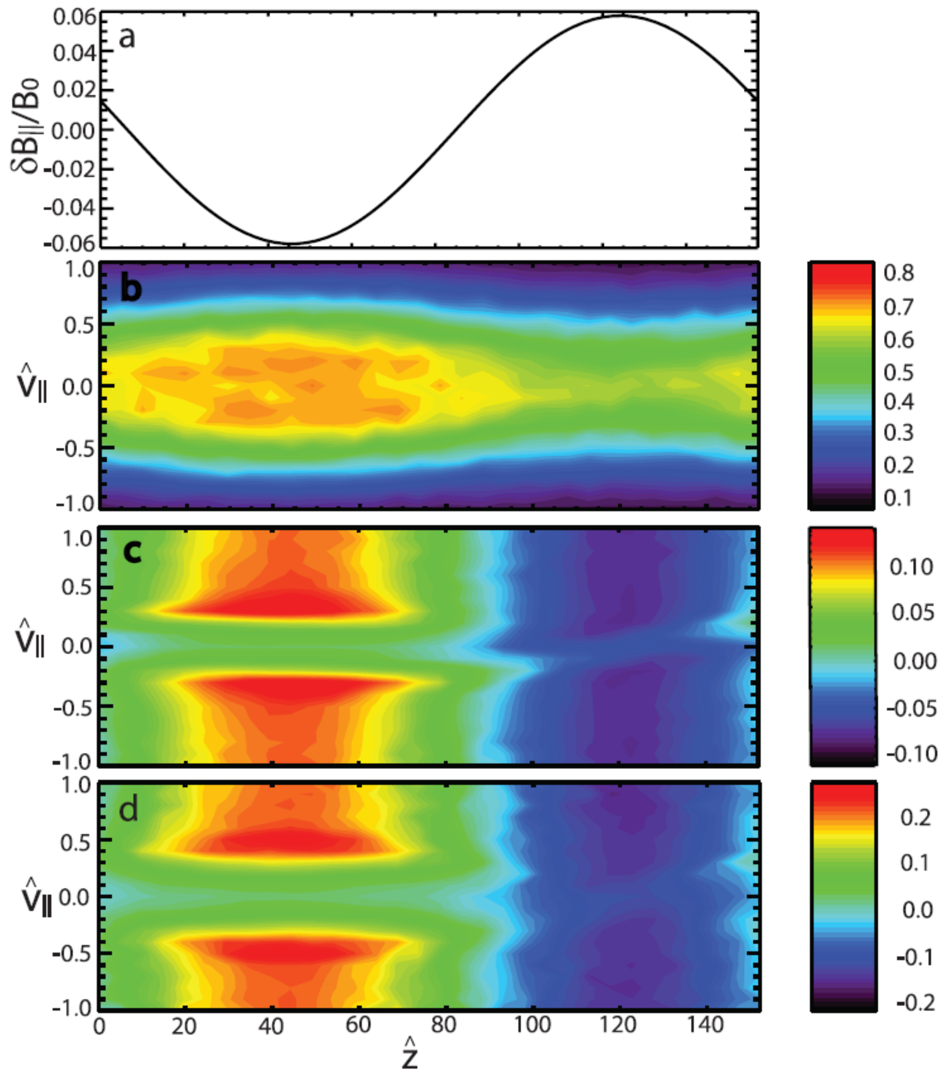

Figure 2. The island formation of the distribution function in the phase-space at $t * \Omega_i = 2250$ (the cross in Figure 1a). (a) The amplitude of the perturbed parallel magnetic field. (b) The distribution function $f = f_0 + \delta F_i$ in the phase-space. (c and d) The normalized perturbed distribution function $\delta F_i/f_0$ taken for $\hat{\mu} = 1$ and $\hat{\mu} = 2$, respectively.

Simulations in a small domain (15x 2π c/ωpi),using an Eulerian code (no numerical noise)

$\beta_{\parallel}$=15, $T_{\perp}/T_{\parallel}$=1.4 and θ=1.37

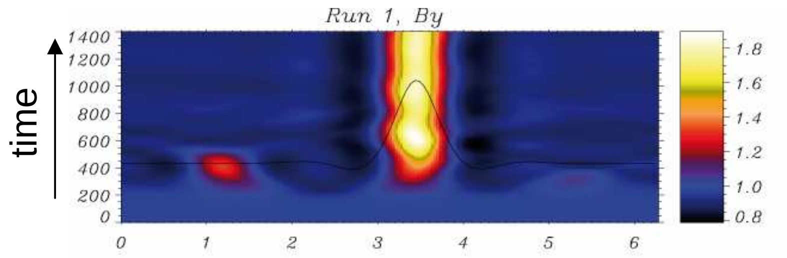

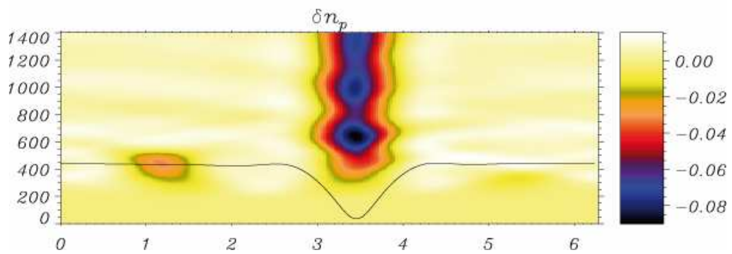

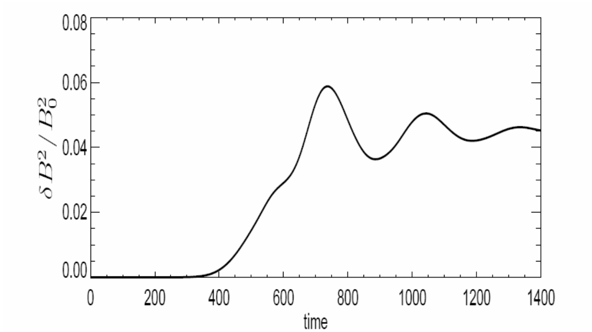

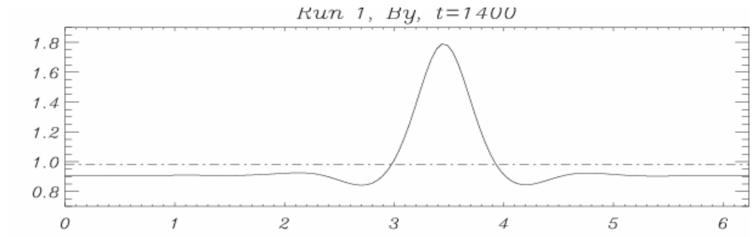

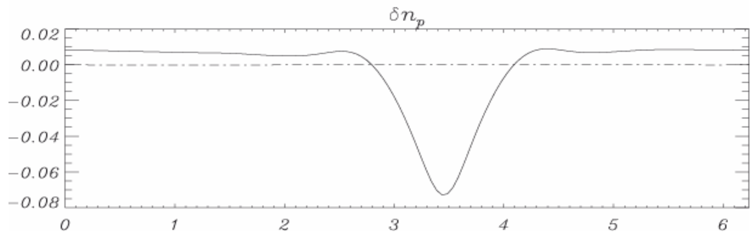

Magnetic hump (and density hole) resulting from the mirror instability, starting from noise.

- In a small domain, the quasi-linear phase is not present.
- Amplitude oscillations, associated with particle trapping.

Magnetic humps form even very close to threshold

$$\beta_{\|} = 6, \quad \theta = 1.463, \quad T_{\perp}/T_{\|} = 1.25$$

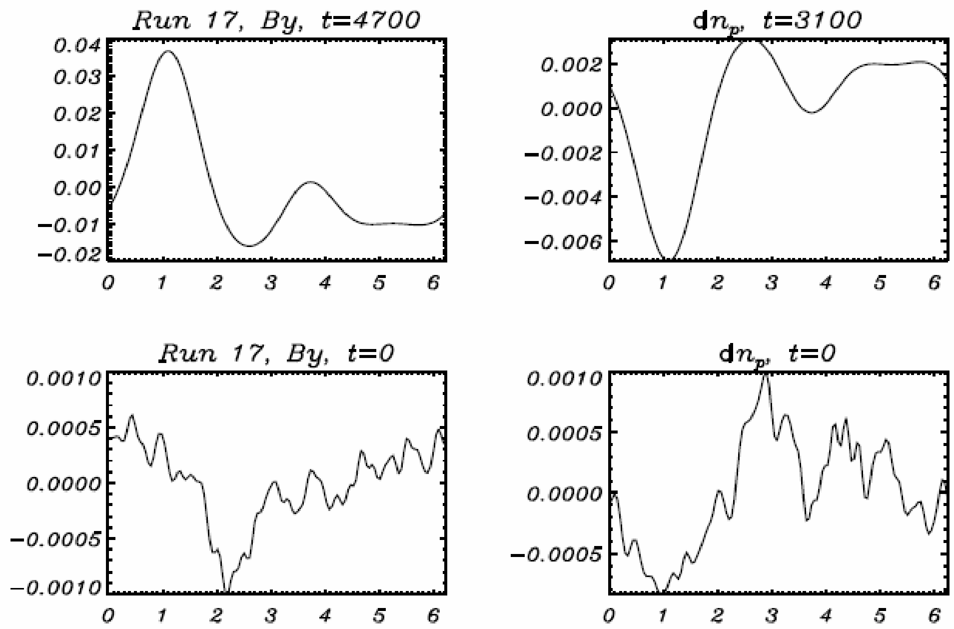

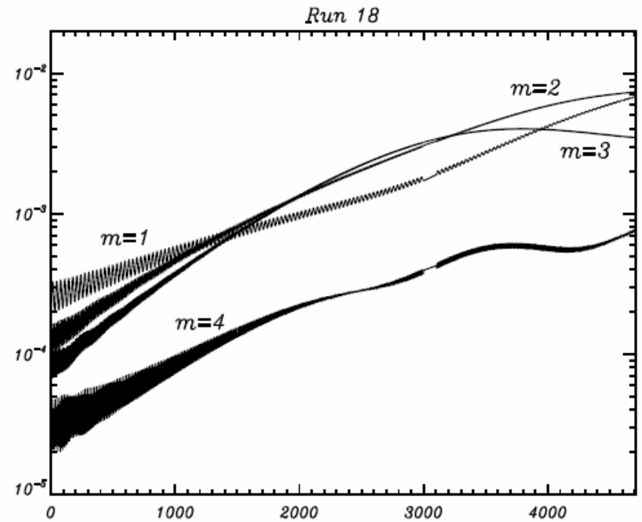

Time evolution of the unstable modes

Growth rate of most unstable mode (m=3) : 0.0017 Ω_i

Distribution function does not display flattening.

No quasi-linear phase.

High resolution in velocity space nevertheless required.

3. Modeling the structure formation

A. Asymptotic expansion *(near a bi-Maxwellian equilibrium)*

Close to threshold, the linearly unstable mirror modes are confined to large scales.

Nonlinear dynamics amenable to a reductive perturbative expansion that isolates mirror modes *(Kuznetsov, Passot & Sulem, PRL, **98,** 235003 ,2007).*

At large scales, kinetic effects (Landau damping and finite Larmor radius corrections) are weak and contribute only linearly in the weakly nonlinear regime supposed to develop near threshold.

This argument is validated by a systematic reductive perturbative analysis performed on the Vlasov-Maxwell system *(Califano et al. JGR **113**, A08212, 2008).*

For the sake of simplicity, assume cold electrons with negligible inertia.

Equation governing the proton velocity (derived from Vlasov equation)

$$\frac{du_p}{dt} + \frac{1}{\rho_p}\nabla\cdot\mathbf{p}_p - \frac{e}{m_p}\left(E + \frac{1}{c}u_p\times B\right) = 0$$

Assuming cold electrons with no inertia:

$$E = -\frac{1}{c}\left(u_p - \frac{j}{ne}\right)\times B \quad \text{with} \quad j = (c/4\pi)\nabla\times B$$

$$\mathbf{p}_p = p_\perp\mathbf{n} + p_{||}\boldsymbol{\tau} + \mathbf{\Pi} \quad \text{with} \quad \mathbf{n} = \mathbf{I} - \widehat{b}\otimes\widehat{b} \qquad \boldsymbol{\tau} = \widehat{b}\otimes\widehat{b} \qquad \widehat{b} = B/|B|$$

$$\boxed{\rho\frac{du_p}{dt} = \nabla\left(p_\perp + \frac{|B|^2}{8\pi}\right) + \left(1 + \frac{4\pi}{|B|^2}(p_\perp - p_{||})\right)\frac{(B\cdot\nabla)B}{4\pi} - \widehat{b}\frac{|B|^2}{4\pi}(\widehat{b}\cdot\nabla)\left(1 + \frac{4\pi}{|B|^2}(p_\perp - p_{||})\right) + \nabla\cdot\mathbf{\Pi}}$$

In order to address the asymptotic regime, we rescale the independent variables in the form $X = \sqrt{\varepsilon}x$, $Y = \sqrt{\varepsilon}y$, $Z = \varepsilon z$, $T = \varepsilon^2 t$, where ε measures the distance to threshold, and expand any field φ in the form

$$\varphi = \sum_{n=0} \varepsilon^{n/2}\varphi_{n/2}$$

Scalings of the space and time variables are suggested by the linear instability growth rate near threshold

$$\gamma = |k_z|v_{\text{th}||}\frac{\beta_{||}}{\sqrt{\pi}\beta_\perp}\left[\frac{\beta_\perp}{\beta_{||}} - 1 - \frac{1}{\beta_\perp} - \frac{k_z^2}{k_\perp^2\beta_\perp}\left(1 + \frac{\beta_\perp - \beta_{||}}{2}\right) - \frac{3}{4\beta_\perp}k_\perp^2\rho_L^2\right]$$

(ρ_L: ion Larmor radius)

In particular

$$B_\perp = \varepsilon^{3/2} B_\perp^{(3/2)} + \varepsilon^{5/2} B_\perp^{(5/2)} + \cdots$$
$$B_z = B_0 + \varepsilon B_z^{(1)} + \varepsilon^2 B_z^{(2)} + \cdots .$$

E.B =0
cold electrons
without inertia

$$E_\perp = \varepsilon^{5/2} E_\perp^{(5/2)} + \varepsilon^{7/2} E_\perp^{(7/2)} + \cdots$$
$$E_z = \varepsilon^5 E_z^{(5)} + \varepsilon^7 E_z^{(7)} \cdots .$$

One shows that $\nabla_\perp \times B_\perp^{(3/2)} = 0$. By the divergenceless condition: $\boxed{B_\perp^{(3/2)} = (-\Delta_\perp)^{-1} \nabla_\perp \partial_Z B_z^{(1)}}$.

Defining $b_Z = B_Z^{(1)} + \varepsilon B_Z^{(2)}$ and $\overline{p}_\perp = p_\perp^{(1)} + \varepsilon p_\perp^{(2)}$,

the ion-velocity equation reduces to a **pressure balance equation**

$$\boxed{\nabla \left[\overline{p}_\perp + \frac{B_0}{4\pi} b_z + \epsilon \frac{b_z^2}{8\pi} + \frac{2\varepsilon}{\beta_\perp} \left(1 + \frac{\beta_\perp - \beta_\parallel}{2}\right) p_\perp^{(0)} (\Delta_\perp)^{-1} \partial_{ZZ} b_z \right] + \epsilon \left(\nabla \cdot \Pi\right)_\perp^{(5/2)} = O(\varepsilon^2)}$$

The perpendicular pressure and the gyroviscous force are to be calculated from Vlasov equation

For a biMaxwellian equlibrium:

$$\overline{p}_\perp = \beta_\perp \left(1 - \frac{\beta_\perp}{\beta_\parallel}\right) \frac{B_0 b_z}{4\pi} + \varepsilon \frac{\sqrt{\pi}}{v_{th\,\parallel}} \partial_T \left(- \mathcal{H}\, \partial_Z \right)^{-1} \frac{\beta_\perp^2}{\beta_\parallel} \frac{B_0 b_z}{4\pi}$$
$$- \epsilon p_\perp^{(0)} \left[\frac{9}{4\beta_\perp} r_L^2 \Delta_\perp \frac{b_z}{B_0} + \left(1 - 4\frac{p_\perp}{p_\parallel} + 3\left(\frac{\beta_\perp}{\beta_\parallel}\right)^2 \left(\frac{b_z}{B_0}\right)^2\right] \right.$$

$$\left(\nabla \cdot \Pi\right)_\perp^{(5/2)} = -\frac{3}{4}\left(1 - \frac{\beta_\perp}{\beta_\parallel}\right) p_\perp^{(0)} r_L^2 \Delta_\perp \nabla_\perp \left(\frac{b_Z}{B_0}\right)$$

r_L: ion Larmor radius

In this near-threshold asymptotics,

- time derivative originates from Landau damping
- Landau damping and finite Larmor radius effects arise only linearly

The vanishing of the contribution of zeroth order reproduces the instability threshold.

Dynamical equation obtained at the next order.

Dynamical equation *(assuming a bi-Maxwellian equilibrium):*

$$\boxed{\begin{aligned}\partial_T\Big(\frac{b_z}{B_0}\Big) = \frac{v_{th\,\|}}{\sqrt{\pi}}\frac{\beta_\|}{\beta_\perp}\Big(-\mathcal{H}\partial_Z\Big)\Big\{\frac{1}{\varepsilon}\Big(\frac{\beta_\perp}{\beta_\|}-1-\frac{1}{\beta_\perp}\Big)\Big(\frac{b_z}{B_0}\Big)+\frac{3}{4\beta_\perp}r_L^2\Delta_\perp\Big(\frac{b_z}{B_0}\Big)\\ -\frac{1}{\beta_\perp}\Big(1+\frac{\beta_\perp-\beta_\|}{2}\Big)\Big(\Delta_\perp\Big)^{-1}\partial_{ZZ}\Big(\frac{b_z}{B_0}\Big)-\frac{3}{2}\Big(\frac{1+\beta_\perp}{\beta_\perp^2}\Big)\Big(\frac{b_z}{B_0}\Big)^2\Big\} = O(\epsilon).\end{aligned}}$$

After simple rescaling

$$\boxed{\partial_\tau U = \Big(-\mathcal{H}\partial_\xi\Big)\Big[\sigma U + \Delta_\perp U - \Delta_\perp^{-1}\partial_{\xi\xi}U - 3U^2\Big]}$$

Here, $\sigma=\pm1$, depending on the positive or negative sign of the threshold parameter $\beta_\perp/\beta_\| - 1 - 1/\beta_\perp$.

When the spatial variation are limited to a direction making a fixed angle with the ambient field

$$\boxed{\partial_T U = \widehat{K}_\Xi\left[(\sigma+\partial_{\Xi\Xi})\,U - 3U^2\right]}$$

$\hat{K}_Z = -\mathcal{H}\,\partial_Z$
whose Fourier transform is $|K_Z|$

where Ξ is the coordinate along the direction of variation.

Finite time blowup of the solution

When spatial variations are limited to a direction making a fixed angle with the ambient field:

$$\frac{\partial U}{\partial T} = \widehat{K}_{\Xi}\left[\left(\sigma + \frac{\partial^2}{\partial \Xi^2}\right) U - 3U^2\right]$$

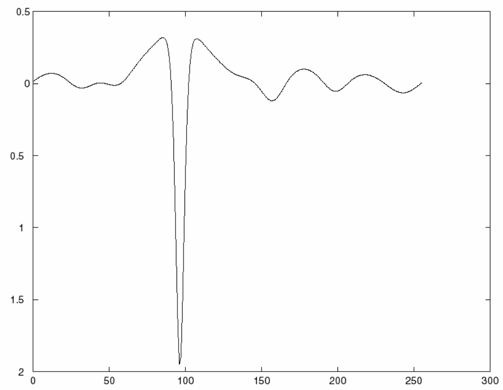

Solution profile near collapse

Integration above threshold (σ>1), with as initial conditions a sine function involving several wavelengths.

After an initial phase of linear instability, formation of a dominant magnetic hole. After a while, solution blows up with a self-similar behavior.

Wave-particle resonance provides the trigger mechanism leading to the linear instability.

Hydrodynamic nonlinearities reinforce the instability, leading to collapse.

Linear FLR effects arrest the linear instability at small scales but cannot cope with hydrodynamic nonlinearities.

At the level of Vlasov-Maxwell eqs, the singularity is the signature of the formation of finite-amplitude structures, through a subcritical bifurcation that cannot be captured perturbatively.

*Kuznetsov, Passot & Sulem, PRL **98**, 235003 (2007).*

Magnetic holes and not humps are obtained !

No stable non-zero stationary solutions to the asymptotic equation

This equation can be written in the form $$\frac{\partial U}{\partial T} = -\widehat{K}_Z \frac{\delta F}{\delta U}$$

where $\widehat{K}_Z = -\mathcal{H}\partial/\partial Z$ is a positive definite operator (whose Fourier transform is $|K_Z|$), and

$$F = \int \left[-\frac{\sigma}{2}U^2 + \frac{1}{2}U\Delta_\perp^{-1}\frac{\partial^2}{\partial Z^2}U + \frac{1}{2}\left(\nabla_\perp U\right)^2 + U^3 \right] d^3R$$

has the meaning of a free energy or a Lyapunov functional. This quantity can only decrease in time, since

$$\frac{dF}{dT} = \int \frac{\delta F}{\delta U}\frac{\partial U}{\partial T} d^3R = -\int \frac{\delta F}{\delta U}\widehat{K}_z \frac{\delta F}{\delta U} d^3R \le 0.$$

dF/dT is *strictly negative* above threshold. It can indeed only vanish for $\frac{\delta F}{\delta U} = \left(\sigma - \Delta_\perp^{-1}\frac{\partial^2}{\partial Z^2} + \Delta_\perp\right)U - 3U^2 = 0.$ (☆)

Above threshold (σ=+1): there is no non-zero solutions of (☆).

Below threshold (σ=-1): solutions exist (in the form of magnetic holes).

In 3D, they correspond to saddle points of the free energy and are thus unstable.

In 1D, the solution is the KdV soliton; the linearized operator near this solution has one neutral mode (associated to space translation) with one node and thus a negative energy level: again it is unstable.

*(Kuznetsov, Passot & Sulem, JETP Letters, **86**, 637, 2007)*

- No steady solutions above threshold
- Unstable solutions below threshold
- Blowup of a small-amplitude initial condition above threshold

⇒ Subcritical bifurcation

Saturated solution is not amenable to a perturbative calculation

Reductive perturbative expansion

performed near bi-Maxwelian equilibrium,
retaining only linear kinetic effects,

predicts that the nonlinear development of the mirror instability leads to the formation of magnetic holes.

Similar observation when using a more comprehensive semi-fluid description:

FLR-Landau fluids *(Passot & Sulem, Phys. Plasmas 14, 082502 (2007)*:
Fluid description obtained by closing the moment hierarchy by means of a closure relation aimed to reproduce the linear kinetic theory near a bi-Maxwellian distribution (include **linear** Landau damping and FLR corrections in the gyrokinetic scaling).

FLR Landau fluids also predict that nonlinear saturation of the mirror instability leads to magnetic holes.

FLR-Landau fluid simulations

(Borgogno, Passot, Sulem, NPG, 14, 373 (2007))

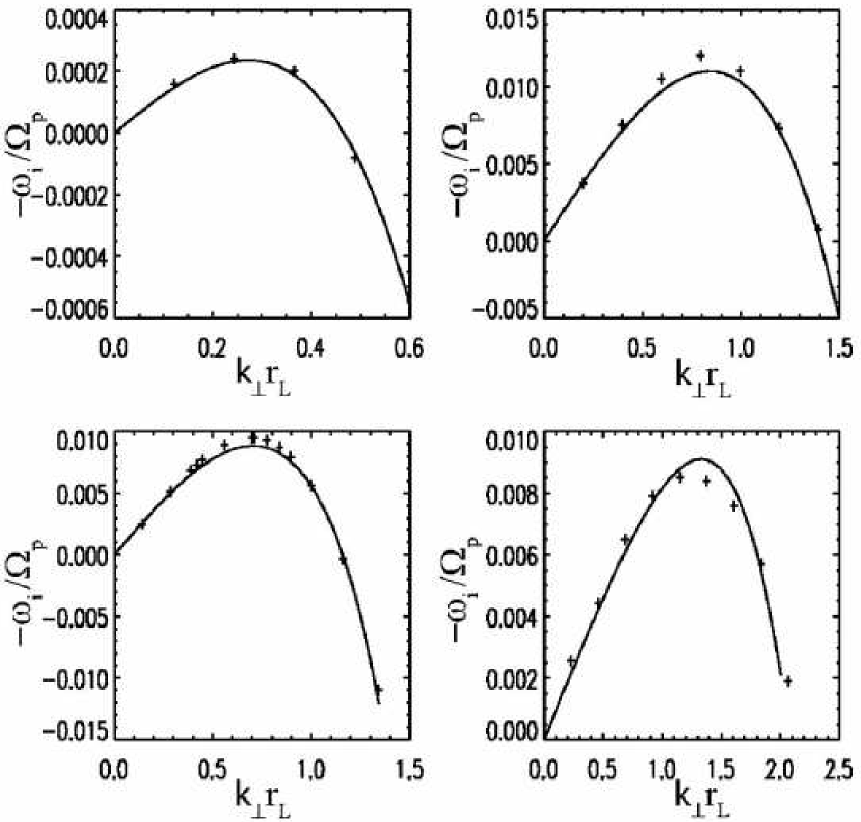

FIG. 10. Normalized growth rate ω_i/Ω_p vs $k_\perp r_L$ for mirror modes with $\beta=5$, $\tau=0.1$, $\theta=\cos^{-1}(0.1)$, $T_{\perp p}/T_{\parallel p}=1.2$, and $T_{\perp e}/T_{\parallel e}=1$ (top, left) and $\beta=2$, $\tau=1$, $\theta=\cos^{-1}(0.1)$, $T_{\perp p}/T_{\parallel p}=2$ and $T_{\perp e}/T_{\parallel e}=1$ (top, right) as a function of $k_\perp r_L$. Same for $\beta=5$, $\tau=1$, $\theta=\cos^{-1}(0.2)$, $T_{\perp p}/T_{\parallel p}=1.4$, and $T_{\perp e}/T_{\parallel e}=1$ (bottom, left). $T_{\perp p}/T_{\parallel p}=1.1$ and $T_{\perp e}/T_{\parallel e}=1.18$ (bottom, right).

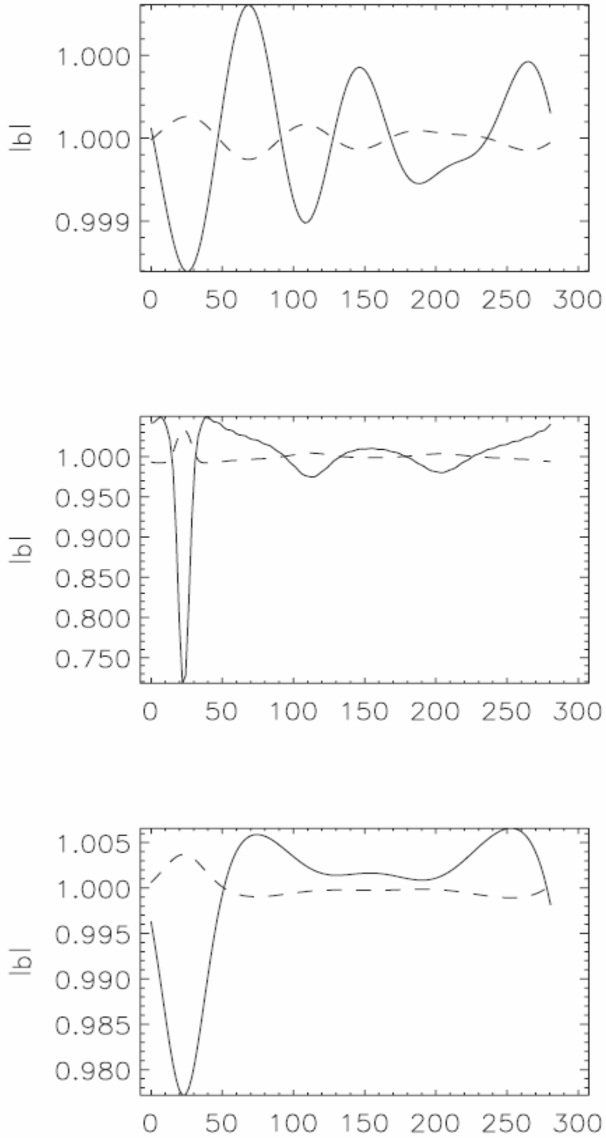

Fig. 2. Snapshots of a simulation illustrating the development of the mirror instability very close to threshold, with $\beta = 5$, $\alpha=88.85°$, $T_{\perp i}/T_{\parallel i}=1.18$ and $T_{\perp e}=T_{\parallel e}=0.05T_{\parallel i}$ at times $t=350 \times 10^3\Omega_i^{-1}$, $t=780 \times 10^3\Omega_i^{-1}$ and $t=850 \times 10^3\Omega_i^{-1}$. Displayed are the magnetic field amplitude (solid line) and the density (dashed line) as a function of space in units of ion inertial length $l_i = \frac{v_A}{\Omega_i}$.

No blow-up

At least one of the two assumptions (bi-Maxwelian equilibrium,linear kinetic effects) is to be challenged.

Extension of the reductive perturbative expansion:

The reductive perturbative expansion near threshold can be extended to any (frozen) smooth equilibrium distribution function $f(v_\|^2, v_\perp)$ provided $\tilde{v} > 0,\ \tilde{r}^2 > 0,\ \text{and}\ \chi > 0)$.

$$\partial_t b = \sqrt{\frac{2}{\pi}}\tilde{v}\,(-\mathcal{H}\partial_z)\left(\Gamma b + \frac{3}{2}\tilde{r}^2\Delta_\perp b - \chi\frac{\partial_z^2}{\Delta_\perp}b - \Lambda b^2\right) \quad (\blacktriangle)$$

$b = \delta B_z(\boldsymbol{r}, t)/B_0$
(normalized parallel magnetic perturbation)

$$\Lambda = \beta_\Lambda - 2\beta_\Gamma + \frac{\beta_\perp}{2} + \frac{1}{2}$$

neglecting the contribution of resonant particles to **Λ** in the case of a smooth distribution fonction

with $\beta_\Lambda = \frac{mn}{p_B}\int \frac{v_\perp^6}{8}\frac{\partial^2 f}{\partial (v_\|^2)^2} d^3v$

For a bi-Maxwellian distribution $\beta_\Lambda = 3/2\beta_\perp^3/\beta_\|^2$, thus **Λ** >0 and the model predicts formation of magnetic holes, while humps are observed in the simulations.

This suggests that the early-time QL dynamics affects the forthcoming formation of the structures.

We are thus led to modify eq.(▲) by assuming that **the coefficients** are not frozen at their initial values but **are evaluated from the instantaneous distribution function given by the QL diffusion equation**.

For consistency, the contribution of resonant particles are to be retained in the estimate of the nonlinear coupling constant.

$$\boxed{\partial_t b = \frac{\sqrt{\frac{2}{\pi}}\tilde{v}}{1 + 2\frac{\tilde{v}}{v_\Lambda}b}(-\mathcal{H}\partial_z)\left(\Gamma b + \frac{3}{2}\tilde{r}^2\Delta_\perp b - \chi\frac{\partial_z^2}{\Delta_\perp}b - \Lambda b^2\right)} \quad (\blacktriangle\blacktriangle)$$

$$v_\Lambda^{-1} = \sqrt{2\pi}\frac{mn}{p_B}\int \frac{v_\perp^6}{8}\delta(v_\|)\frac{\partial^2 f}{(\partial v_\|^2)^2} d^3v$$

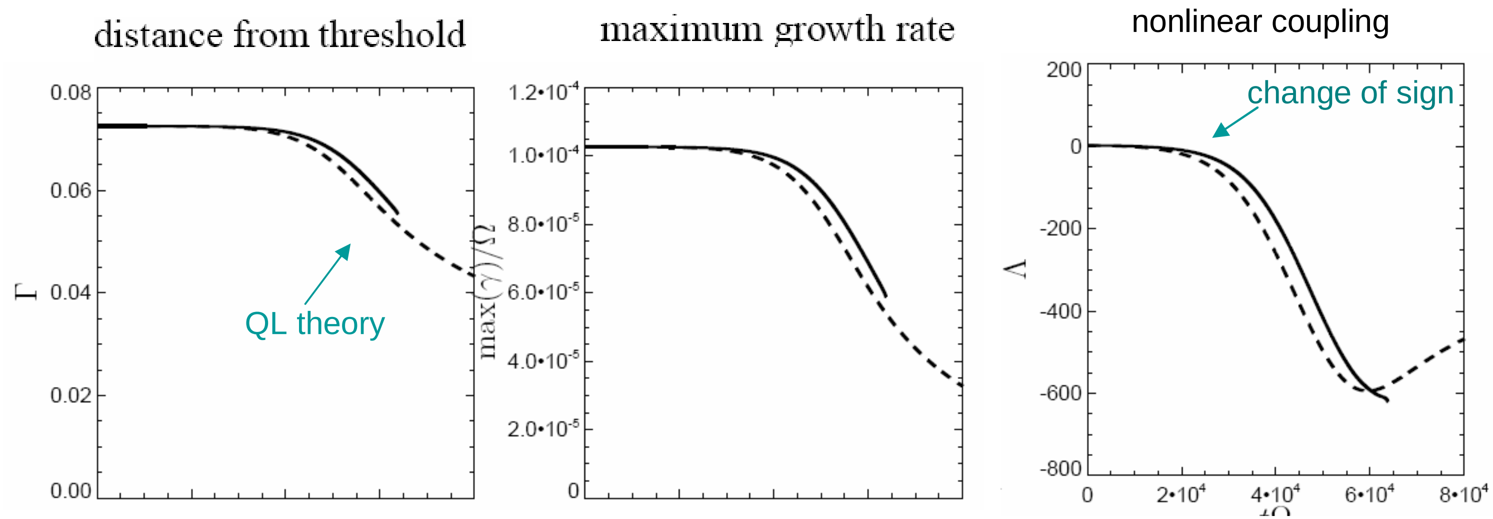

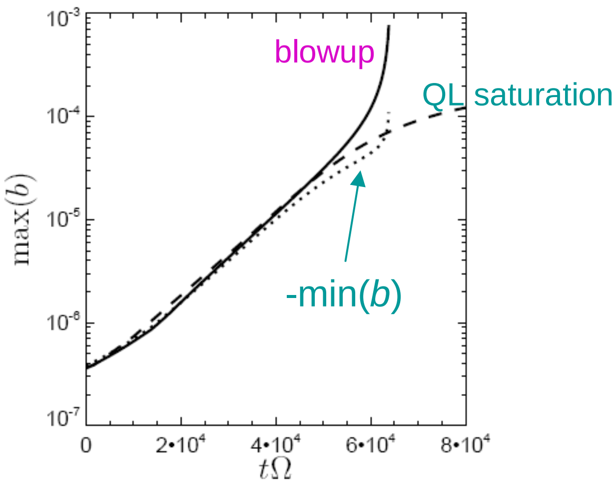

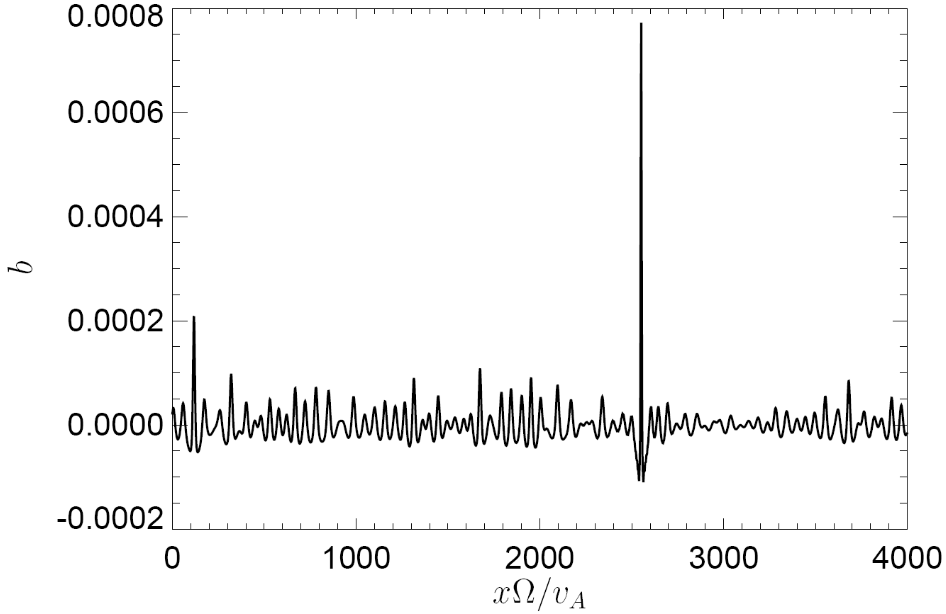

Results of the simulation of eq. (▲▲)

Formation of magnetic humps

The asymptotic equation cannot capture the saturation of the mirror instability.
The asymptotic scaling are broken rather early.

B. Phenomenological modeling of the saturation

I. Models based on particle trapping:

(i) *Pantellini et al. Adv. Space Res.* ***15****, 341 (1995)*
Kivelson and Southwood JGR ***101,*** *17365 (1996)*
Pantellini JGR ***103****, 4789 (1998)*

Assume a separation of the particle distribution into trapped and untrapped components that respond differently to magnetic field variations.
Saturation results from the cooling of trapped particles in magnetic troughs.

Usually predict deep magnetic holes and are hardly consistent with the presence of magnetic humps (only predicted for exceptionally high values of β); Bi-stability not addressed.

(ii) *Pokhotelov et al. JGR* ***113****, A04225 (2008):* phenomenological modeling of particle trapping by a prescribing flattening of the parallel distribution function on a range that extends with the strength of the magnetic perturbation. This leads to a renormalization of the time derivative (associated with the quenching of the Landau resonance).

$$\left(1 - \frac{2}{\pi}\arctan\frac{|h|^{1/2}}{\gamma}\right)\frac{\partial h}{\partial \tau} = \hat{k}_{\xi}\left[\left(1 + \frac{\partial^2}{\partial \xi^2}\right)h - h^2\right]$$

Prevents wave collapse.
The stationary solutions still have the form of KdV solitons.

Only holes can result from this approach.

II. Effect of **variation of the local ion Larmor radius:**

when phenomenologically supplemented to the asymptotic equation,
it makes the model **consistent with Vlasov-Maxwell simulations.**

Motivation:

In regions of weaker magnetic field (and/or large $T_\perp$), ion Larmor radius is larger, making the stabilizing effects of finite radius corrections more efficient than in the linear regime. Consequently, mirror instability is more easily quenched in magnetic field minima than in maxima, making magnetic humps more likely to form in the saturating phase of the mirror instability.

Assume a bi-Maxwellian equilibrium

$$\boxed{\partial_\tau U = \left(-\mathcal{H}\partial_\xi\right)\left[\sigma U + \Delta_\perp U - \Delta_\perp^{-1}\partial_{\xi\xi}U - 3U^2\right]}$$

$$\boxed{\Delta_\perp U \to \frac{1}{1+\alpha U}\Delta_\perp U + \frac{4}{9}\frac{\nu}{(1+\alpha U)^2}\Delta_\perp^2 U}$$

ν (taken equal to 0.01) is related to the size of the box

$$\alpha = \frac{2\beta_\perp}{1+\beta_\perp}\left[\beta_\perp\left(\frac{T_\perp}{T_\parallel}-1\right)-1\right]$$

Singularity is arrested

Using conservation of magnetic moment,

$$\rho_L^2 \propto T_\perp/|B|^2 \propto 1/|B| \approx 1/B_z$$

Furthermore, in addition to Laplacian which results from the leading order expansion of a nonlocal operator associated with FLR corrections, we also retain the next order contribution.

Evolution after saturation of linear instability

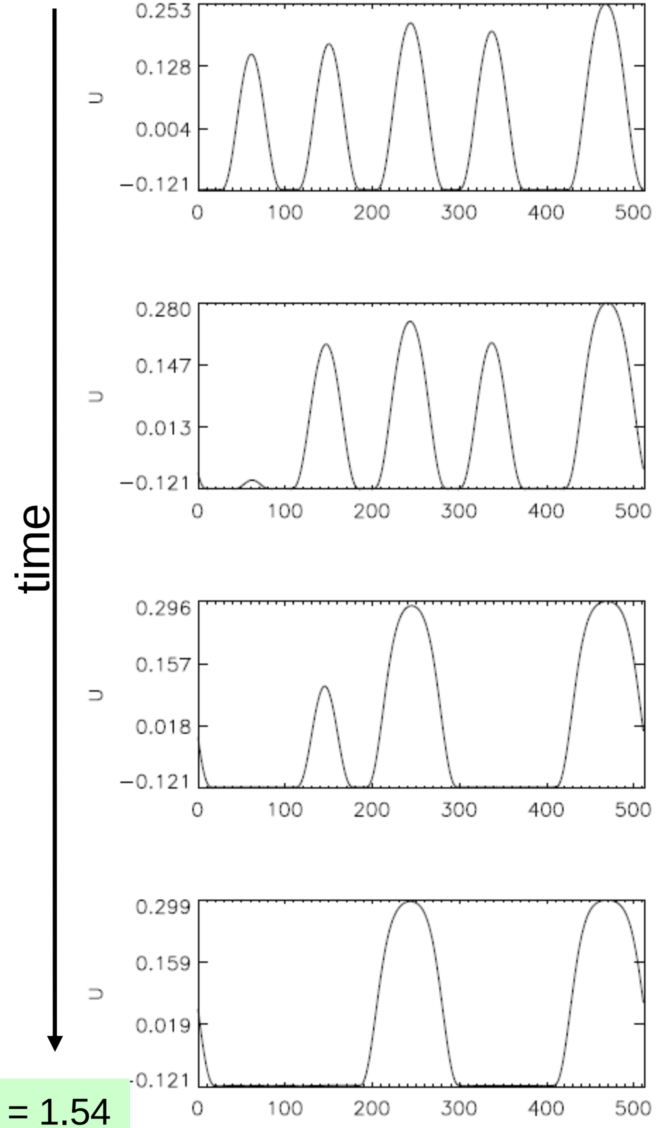

$\sigma\alpha$ = 1.54

Coarsening of magnetic humps resulting from the mirror instability in the framework of the phenomenological model.

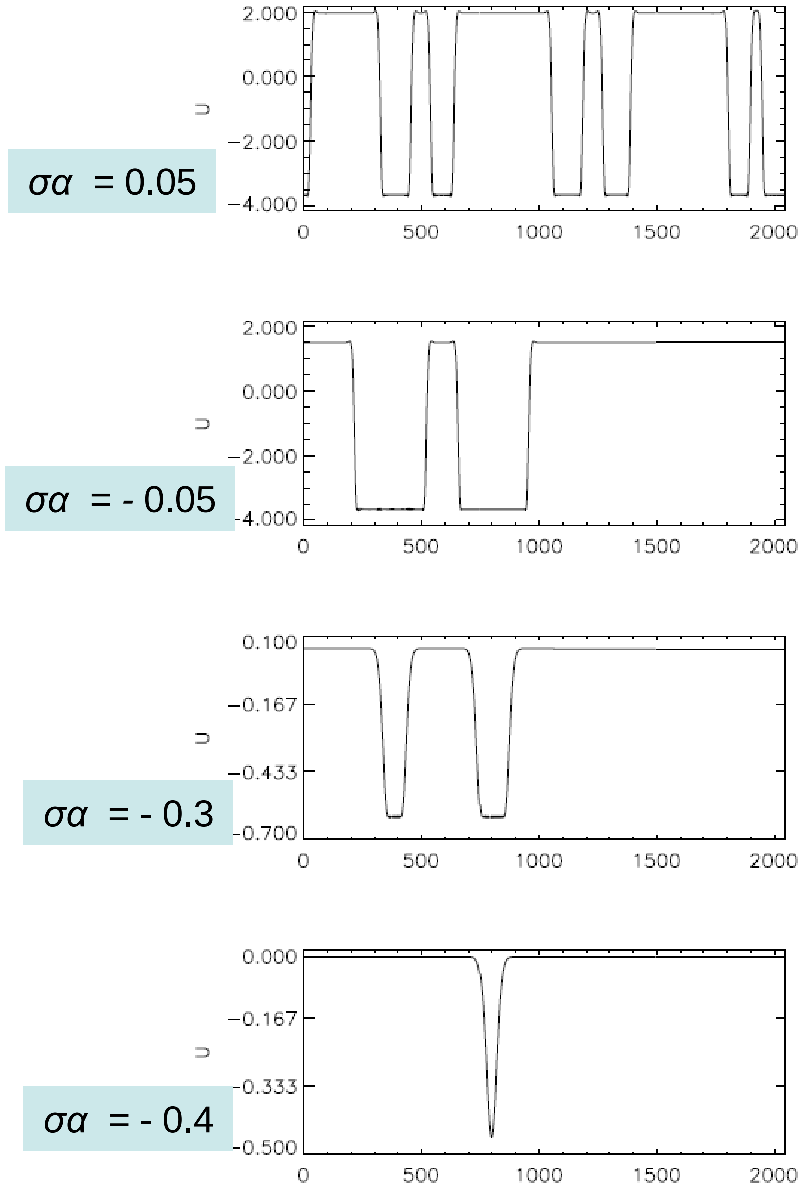

Magnetic holes predicted by the phenomenological model initiated by a random noise of small amplitude when $\sigma > +1$ and of large amplitude when $\sigma < -1$.

Skewness of magnetic fluctuations in the quasi-stationary regime

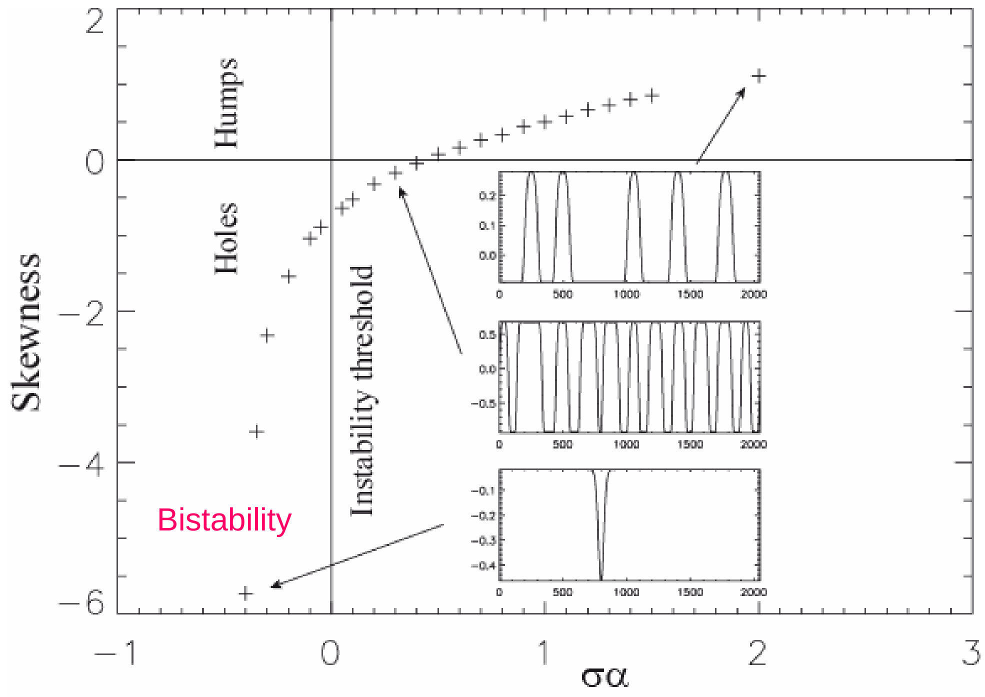

Figure 10. Variation of the skewness with the parameter $\sigma\alpha$, as predicted by the phenomenological model.

I.C.: small-amplitude random noise in supercritical regime
large-amplitude random noise in subcritical regime

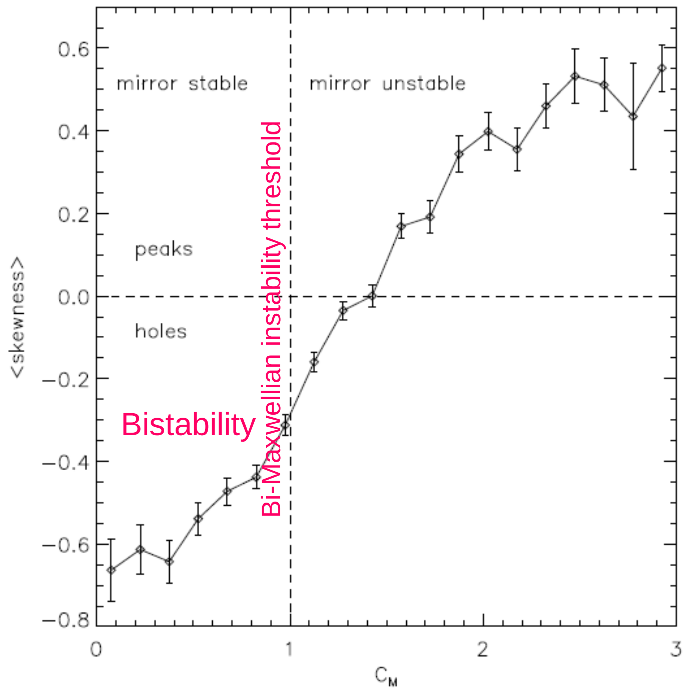

$$C_M = \beta_{p\perp}\left(\frac{T_{p\perp}}{T_{p\|}} - 1\right)$$

Cluster data : statistic of structures observed in the magnetosheath.

Génot et al., Ann. Geophys. **27,** 601 (2009).

4. Formation of magnetic holes when starting with large initial perturbations

Subcritical solutions (i.e. below threshold)

Model simulation

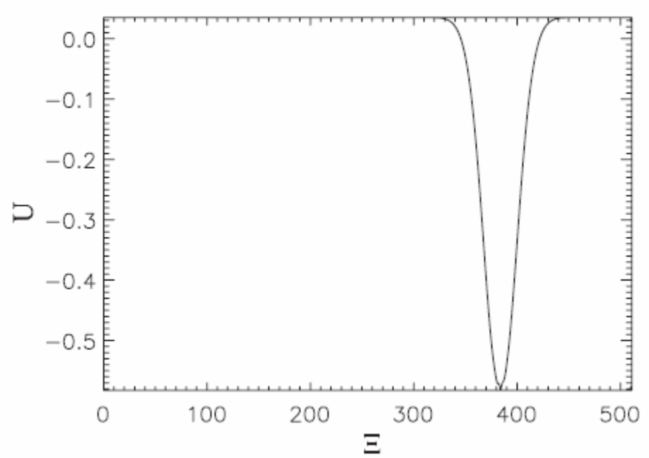

FIG. 4. Quasistatic solution of the saturated equation for $\sigma = -1$, $\nu = 0.01$, and $\alpha = 0.32$, obtained with large initial perturbations.

Vlasov simulation in a small domain

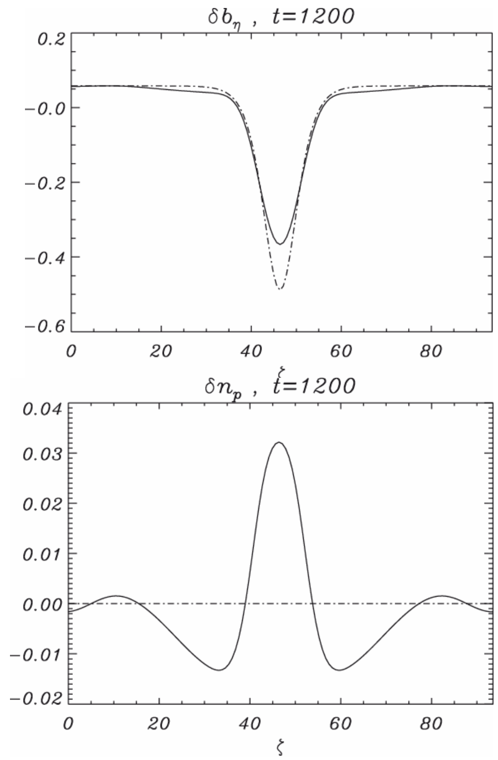

$$\beta_{\parallel} = 6, \quad \theta = 1.463, \quad T_{\perp} = T_{\parallel}$$

Large-amplitude magnetic holes survive even far **below threshold**.

Magnetic humps do not survive

PIC hybrid simulations at moderate β below threshold (Baumgärtel, Sauer & Dubinin, GRL, 2003)

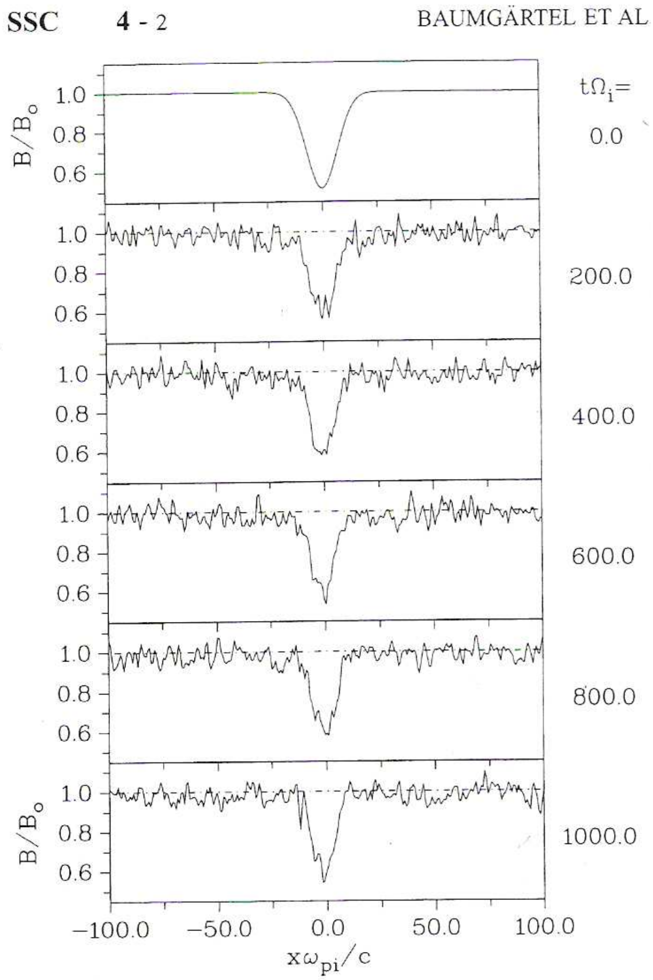

Figure 1. Space-time evolution of a magnetic depression in an otherwise uniform, collisionless, isotropic high-β plasma with $\beta_i = 2.5$, $\beta_e = 1$, $\theta = 80°$. The initial perturbation is prescribed as $\delta B_z/B_0 = -0.5 \exp(-x^2/h^2)$ with $h = 10\ c/\omega_{pi}$; δB_y is set to zero at $t = 0$.

A localized magnetic perturbation in the form of a finite-amplitude hole persists

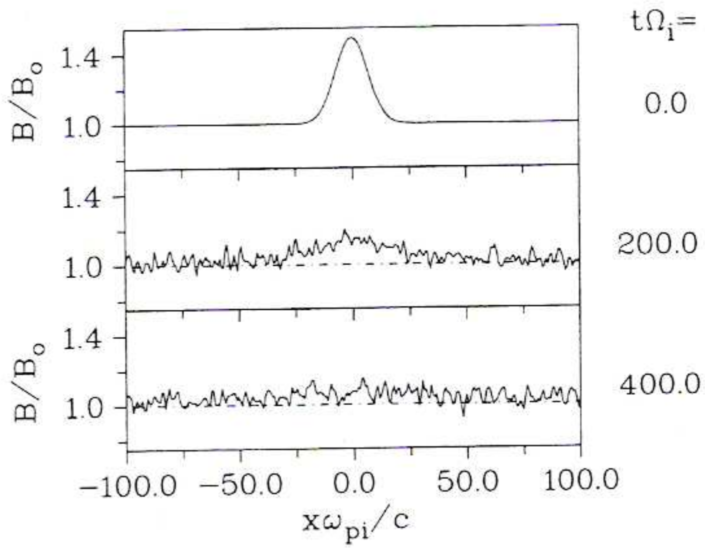

Figure 3. Space-time evolution of a magnetic compression $\delta B_z/B_0 = 0.5 \exp(-x^2/h^2)$, other parameters the same as in Figure 1.

A localized magnetic perturbation in the form of a finite-amplitude hump relaxes

Eulerian Vlasov simulations in a small domain for **large-amplitude initial perturbations above threshold**

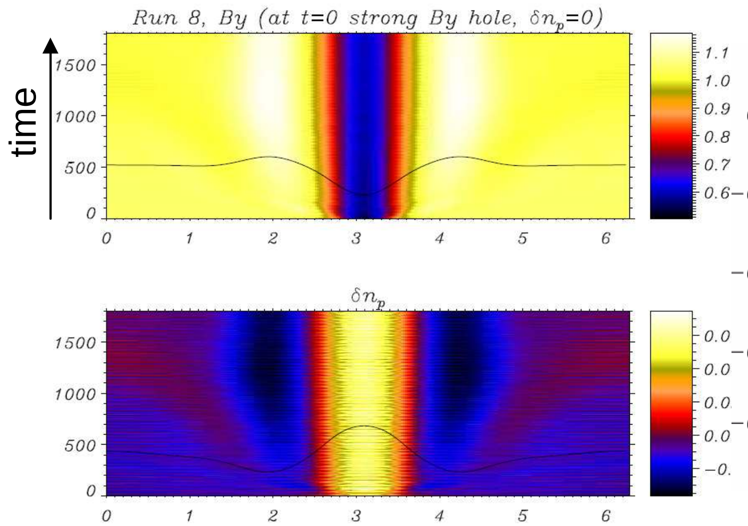

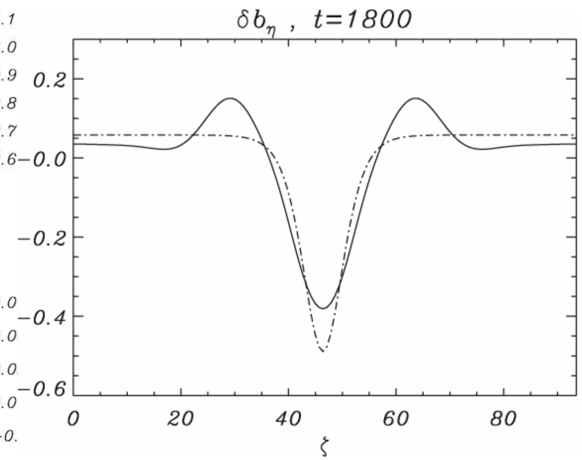

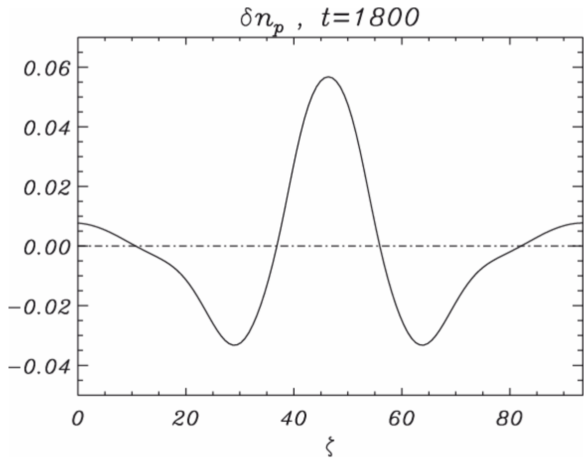

Note the overshoot

Magnetic hole (and density hump), starting with a large amplitude magnetic field depression, above threshold.

Domain size: 15x $2\pi\ c/\omega_{pi}$, with $\beta_{\|}=6$, $T_{\perp}/T_{\|}=1.2$ and $\theta=1.463$

Overshoot

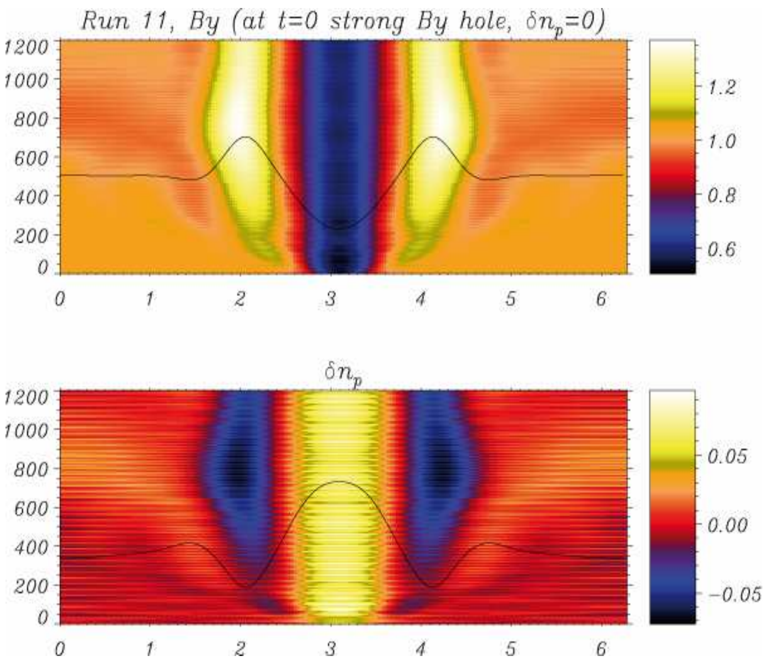

$$\beta_{||} = 6, \quad \theta = 1.463, \quad T_{\perp}/T_{||} = 1.5$$

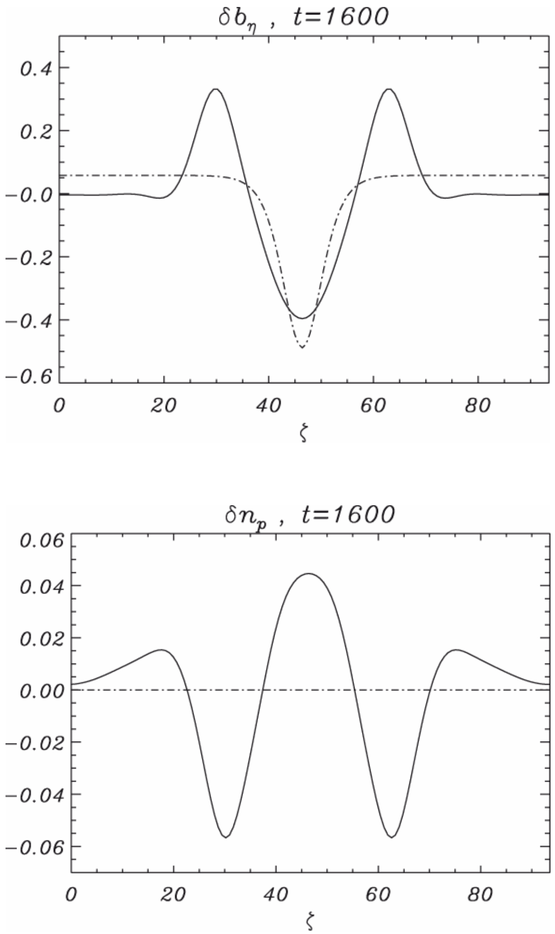

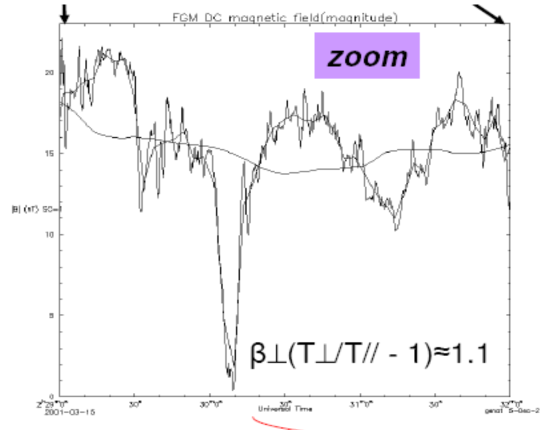

Cluster observation
(Génot et al., AGU 2006)

Large-amplitude magnetic holes are found to be stable solutions
even far above threshold.

Mirror structures are different from soliton solutions:

Magnetic field component perpendicular to the plane (**k, B**$_o$) is symmetric with respect to the center of the magnetic hole.

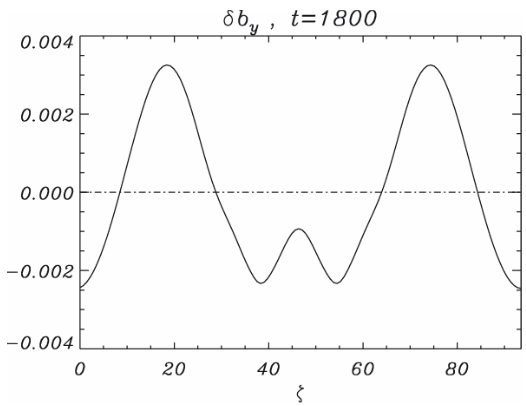

hodograph

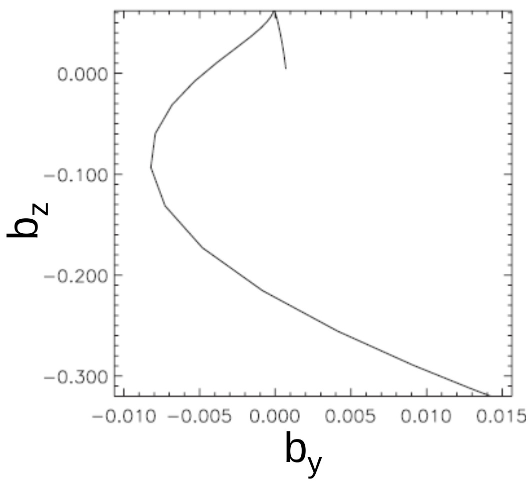

Differently, soliton models based on anisotropic Hall-MHD *(Stasiewicz 2004, Mjolhus 2006)* predict an antisymmetric b_y profile.

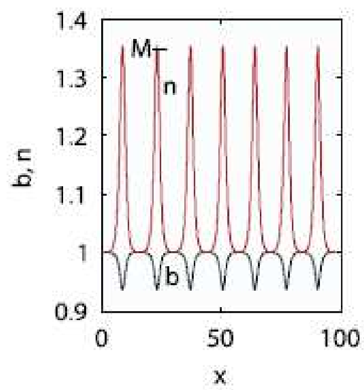

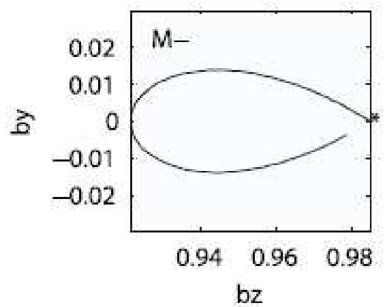

Stasiewicz, JGR **110**, A03220 (2005)

Formation of **magnetic holes** from small-amplitude noise in a mirror unstable plasma

PIC simulation far from threshold starting form random noise.
Early-formed humps transform into holes.

1024 cells with 500 000 particles/cell; Domain size=1024 c/ω_{pi}
Growth rate: 0.156 Ω_p^{-1}

$\theta_{kB} = 50.5^o$ (most unstable angle)

$\beta_{p\|} = 1 \quad \beta_{p\perp} = 4$

$\beta_e = 10^{-2}$

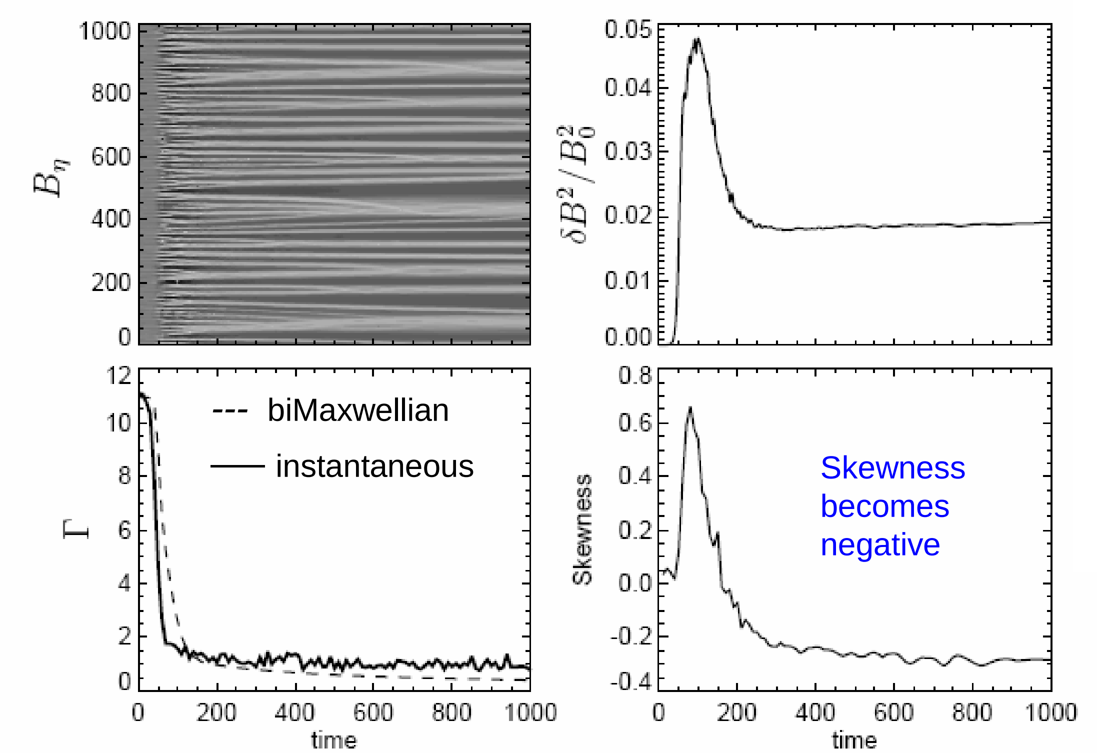

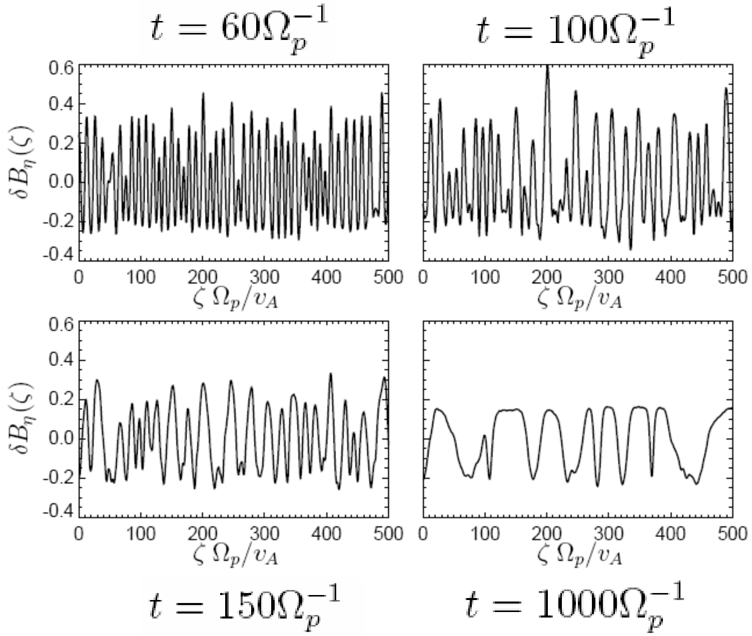

(quarter of the box)

Distance to threshold remains slightly positive.
The system is continuously stirred and coarsening is less efficient.
In particular, there are no isolated structures.

Late transition from magnetic humps to magnetic holes

β is decreasing, which favours nonlinear stability of magnetic holes.

No such transition at larger β (e.g. $\beta_{p\|} = 2$).

Resulting magnetic holes:

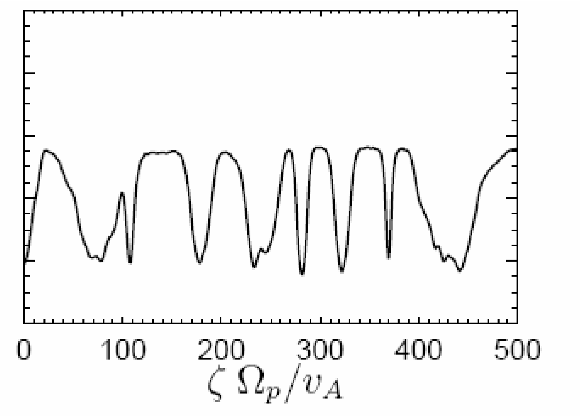

Qualitative similarity with Ulysses measurements in the magnetosheath of Jupiter (Erdös & Balogh 1996):

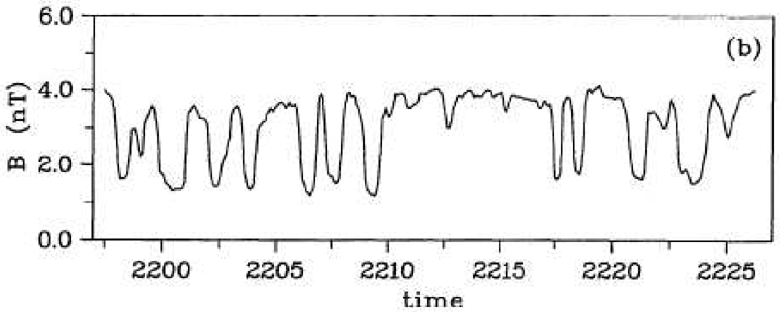

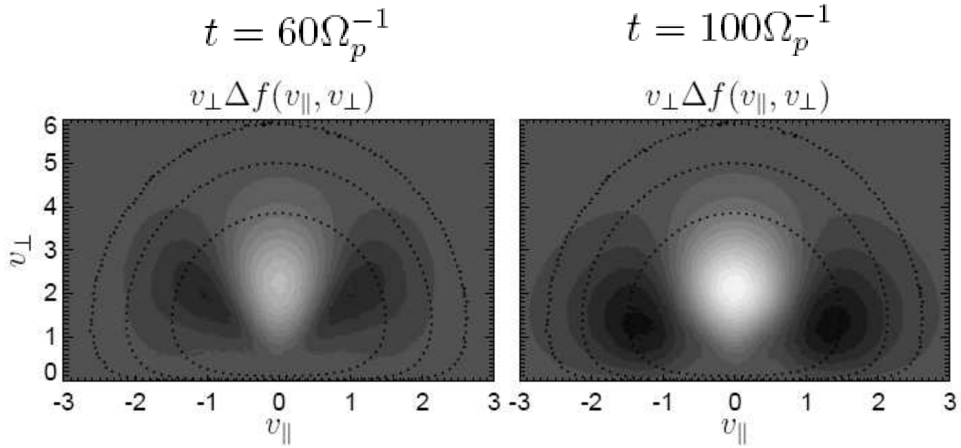

Space-integrated distribution function variation

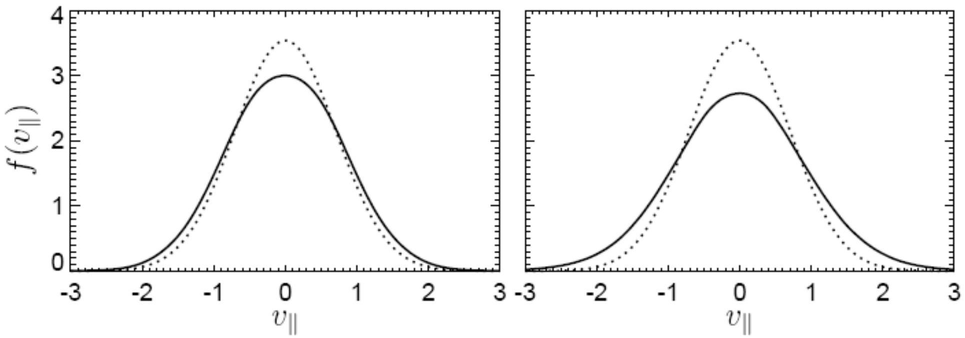

Space-integrated parallel distribution function

The distribution function remains close to bi-Maxwellian.

No flattening of the distribution function.

5. Summary

- Numerical integrations in a large domain of VM equations demonstrate the existence of an early phase described by quasi-linear theory, followed by a regime where coherent structures form.

- In a small domain, no quasi-linear phase but significant oscillations due to particle trapping.

- **The structures resulting from the saturation of the mirror instabilty are magnetic humps.**

- Stable solutions in the form of large-amplitude magnetic holes exist both above and below threshold.

- Holes can also form in the late evolution of an extended system when initialized far from threshold.

- Reductive perturbative expansion of VM eqs near threshold leads to an equation with a finite-time singularity, signature of a **subcritical bifurcation**. Nature of the structures depends on the equilibrium distribution function. An early QL phase can provide the conditions for the formation of magnetic humps.

- A phenomenological modeling retaining ion Larmor radius variations predicts the formation of *saturated* magnetic humps above threshold and existence of stable large-amplitude magnetic holes mainly below threshold, in agreement with observations and numerical simulations.

Refs: *Kuznetsov, Passot & Sulem, PRL 98, 235003 (2007); JETP Letters 86, 637 (2008)*
Califano, Hellinger, Kuznetsov, Passot, Sulem & Travnicek, JGR 113, A08219 (2008).
Hellinger, Kuznetsov, Passot, Sulem & Travnicek,GRL, 34, xxxx, DOI:10.1029/2008GL036805. in press.
Génot, Budbik, Hellinger, Passot, Belmont, Travnicek, Sulem, Lucek & Dandouras, Ann. Geophys. 27, 601 (2009).

6. Open questions

- Would it be possible to retain nonlinear FLR effects and the influence of trapped particles within an asymptotic theory?
- Are there conditions where mirror instability saturates by quasi-linear effects?
- Can one observe, very close to threshold, the signature of the singularity predicted by the reductive perturbative expansion ?
- How to understand quantitatively the transition from humps to holes observed in large-box simulations far from threshold?
- Perform Vlasov-Maxwell simulations in two or three dimensions.
- What is the role of the mirror structures on the magnetopause boundary?
  Can they trigger micro-reconnection events?